

THE UNIVERSITY OF MICHIGAN
ANN ARBOR, MICHIGAN

QUARTERLY PROGRESS REPORT NO. 3

FOR

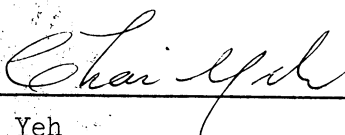
BASIC RESEARCH IN MICROWAVE DEVICES AND QUANTUM ELECTRONICS

This report covers the period November 1, 1963 to February 1, 1964

Electron Physics Laboratory
Department of Electrical Engineering

By: H. K. Detweiler
M. E. El-Shandwily
B. Ho
J. E. Rowe
C. Yeh

Approved by:



C. Yeh
Project Engineer

Approved by:



J. E. Rowe, Director
Electron Physics Laboratory

Project 05772

DEPARTMENT OF THE NAVY
BUREAU OF SHIPS
WASHINGTON 25, D. C.
PROJECT SERIAL NO. SRO080301, TASK 9391
CONTRACT NO. N0bsr-89274

March, 1964

engn

UNR0567

v.3

ABSTRACT

Generation and Amplification of Coherent Electromagnetic Energy in the Millimeter and Submillimeter Wavelength Region

An experimental low-frequency model of the frequency multiplier has been designed. A scheme of feedback to enhance the transfer efficiency is included. The tube is in the final stage of assembly and alignment.

Difficulties in loading a helix designed to operate at 30 Gc into a BeO tube have not been fully resolved. Experimental data indicates that a material having a higher resiliency than tungsten should be used for the helix.

Analysis of Amplitude-and Phase-Modulated Traveling-Wave Amplifiers

The analysis of the operation of the TWA with a multi-frequency input has been extended to account for the multivalued nature of the electron velocity in the beam. Boltzmann's transport equation is used to describe the kinematics of the electron beam.

Study of a D-c Pumped Quadrupole Amplifier

A comprehensive study of the coupling mechanism between the various modes of operation of a d-c pumped transverse wave device has been made by means of the coupled-mode theory. Equations for the gain for the various modes and different pump fields are computed and compared.

TABLE OF CONTENTS

	<u>Page</u>
ABSTRACT	iii
LIST OF ILLUSTRATIONS	vi
LIST OF TABLES	viii
PERSONNEL	ix
ARTICLES PUBLISHED DURING THE LAST QUARTER	x
1. GENERAL INTRODUCTION	1
2. GENERATION AND AMPLIFICATION OF COHERENT ELECTROMAGNETIC ENERGY IN THE MILLIMETER AND SUBMILLIMETER WAVELENGTH REGION	2
2.1 Study of the Interaction Between an Electron Beam and a Dielectric Circuit	2
2.2 Study of Frequency Multiplication in an Angular Propagating Circuit	2
2.2.1 Construction of the Experimental Tube	2
2.2.1a The Electron Gun	4
2.2.1b The Input Coupler	4
2.2.1c The Multiplier Cavity	4
2.2.1d The Feedback Coupler	5
2.2.1e The Collector	5
2.2.2 Future Work	5
2.3 Investigation of High-Thermal-Conductivity Materials for Microwave Devices Above X-Band	5
2.3.1 Introduction	5
2.3.2 Experimental Effort	6
2.3.3 Future Work	7
3. ANALYSIS OF AMPLITUDE AND PHASE-MODULATED TRAVELING-WAVE AMPLIFIERS	8
3.1 Introduction	8
3.2 Method of Analysis	8
3.3 Solution of the Equations	18
3.4 Program for the Next Quarter	40

	<u>Page</u>
4. STUDY OF A D-c PUMPED QUADRUPOLE AMPLIFIER	40
4.1 Introduction	40
4.2 Coupled-Mode Equations of Beam Dynamics	41
4.3 Coupled-Mode Analysis of D-c Pumped Quadrupole Amplifiers	43
4.3.1 General Procedure of the Analysis	43
4.3.2 Staggered Quadrupole Amplifier	46
4.3.3 Other Pumping Fields	60
4.3.3a Twisted Quadrupole Pump Structure	60
4.3.3b Periodic Ring Quadrupole Structure	62
4.3.3c Electrostatic Slot Pump Field Structure	64
4.3.4 Gain Computation of the D-c Pumped Amplifiers	65
4.4 Future Work	73
5. GENERAL CONCLUSIONS	73

LIST OF ILLUSTRATIONS

<u>Figure</u>		<u>Page</u>
2.1	Assembly Drawing of Cyclotron-Frequency Multiplier.	3
4.1	Geometrical Configurations of a Staggered Quadrupole Pump Structure.	47
4.2	Phase Constant vs. Pumping Parameter M for the Fast Cyclotron Wave in a Staggered Quadrupole Pump Structure. $\beta_q = 2\beta_c$, Fast and Slow Cyclotron Wave Interaction.	52
4.3	Amplitude Gain vs. Pumping Parameter M for the Fast Cyclotron Wave in a Staggered Quadrupole Pump Structure. $\beta_q = 2\beta_c$, Fast and Slow Cyclotron Wave Interaction.	53
4.4	ω - β Plot of the Cyclotron-to-Synchronous Wave Interaction in a Staggered Quadrupole Pump Structure, Passive Coupling.	57
4.5	ω - β Plot of the Cyclotron-to-Synchronous Wave Interaction in a Staggered Quadrupole Pump Structure, Active Coupling.	58
4.6	Phase Constant vs. Pumping Parameter M for the Fast Cyclotron Wave in a Staggered Quadrupole Pump Structure. $\beta_q = \beta_c$ Fast Cyclotron-to-Synchronous Wave Interaction.	59
4.7	Geometrical Configurations of (a) Twisted Quadrupole-Type, (b) Periodic Ring-Type and (c) Periodic Slot-Type of Quadrupole Pump Structures.	61
4.8	Gain vs. Pump Voltage for Cyclotron-to-Cyclotron Type of Interaction in Different Pump Fields for $V_o = 100$ Volts, $\beta_a = 1$, and $n = 4$.	67
4.9	Gain vs. Pump Voltage for Synchronous-to-Synchronous Type of Interaction in Different Pump Fields for $V_o = 100$ Volts, $\beta_c = 1$, and $n = 4$.	68
4.10	Gain vs. Pump Voltage for Cyclotron-to-Synchronous Type of Interaction in Different Pump Fields for $V_o = 100$ Volts, $\beta_c = 1$, and $n = 4$.	69

Figure

Page

4.11

Gain vs. $\beta_c a$ for Synchronous-to-Synchronous
Type of Interaction in Different Pump Fields
for $V_p/V_o = 4$, $L = 40$ cm and $U_o = 4.2 \times 10^6$
m/sec.

72

LIST OF TABLES

<u>Table</u>		<u>Page</u>
4.1	Gain Equations for Various Types of Beam Interaction and Different Types of Pump Fields	70

PERSONNEL

<u>Scientific and Engineering Personnel</u>		<u>Time Worked in</u> <u>Man Months*</u>
G. Hok	Professor of Electrical Engineering	.30
C. Yeh	Associate Professor of Electrical Engineering	1.16
M. El-Shandwily	Research Associate	1.36
H. Detweiler	Research Assistants	1.36
B. Ho		1.36
<u>Service Personnel</u>		5.27

* Time Worked is based on 172 hours per month.

ARTICLES PUBLISHED DURING THE LAST QUARTER

C. Yeh, J. C. Lee, "Feedback in Cyclotron-Wave Frequency Multiplier",
Proc. IEEE, vol. 52, No. 3, p. 314; March, 1964.

INTERIM SCIENTIFIC REPORT NO. 3

FOR

BASIC RESEARCH IN MICROWAVE DEVICES AND QUANTUM ELECTRONICS

1. General Introduction (C. Yeh)

The purpose of this project is to investigate new ideas in the area of microwave devices and quantum electronics. The program is envisioned as a general and flexible one under which a wide variety of topics may be studied. At present, the following areas of investigation are in progress:

A. Study of frequency multiplication in an angular propagating circuit. A tube based upon the analysis described in the preceding reports, No. 1 and No. 2, is designed. The construction of this tube is nearly completed.

B. Investigation of high-thermal-conductivity materials for microwave devices above X-band. The work on developing a technique to braze a 30 Gc helix to a BeO tube is continuing.

C. Analysis of amplitude- and phase-modulated traveling-wave amplifier. The theory has been extended to cover the possibility of having multivalued functions of electron velocity in the beam.

D. Study of a d-c pumped quadrupole amplifier. A comprehensive study of the d-c pumped transverse wave device has been made by means of the coupled-mode theory. Some interesting aspects of the coupling mode are discussed.

The work on the study of interaction between an electron beam and a dielectric circuit has been temporarily suspended.

2. Generation and Amplification of Coherent Electromagnetic Energy in the Millimeter and Submillimeter Wavelength Region

2.1 Study of the Interaction Between an Electron Beam and a Dielectric Circuit (G. Hok)

The work on this task has been temporarily suspended because of shortage of available manhours.

2.2 Study of Frequency Multiplication in an Angular Propagating Circuit (C. Yeh, B. Ho)

2.2.1 Construction of the Experimental Tube. The design of the experimental frequency multiplier tube using a multipole cavity as the multiplier element and a feedback scheme to enhance the conversion efficiency was presented in Quarterly Progress Report No. 2. During the present period, progress has been made in the actual construction of such a tube. The design data are as follows:

Input frequency	696.3 mc/s
Output frequency	2785.0 mc/s
Magnetic flux density	250 gauss
Beam voltage	20 volts
Beam current	250 microamperes
Maximum r-f beam power	770 mw
Maximum beam cyclotron radius	17/32 inch
Input coupler plates	2-1/4" x 9/16"
Input coupler separation	9/16"
Feedback coupler plates	1-15/16" x 31/64"
Feedback coupler separation	31/64"

The detailed diagram of the assembly of the cyclotron frequency multiplier is shown in Fig. 2.1.

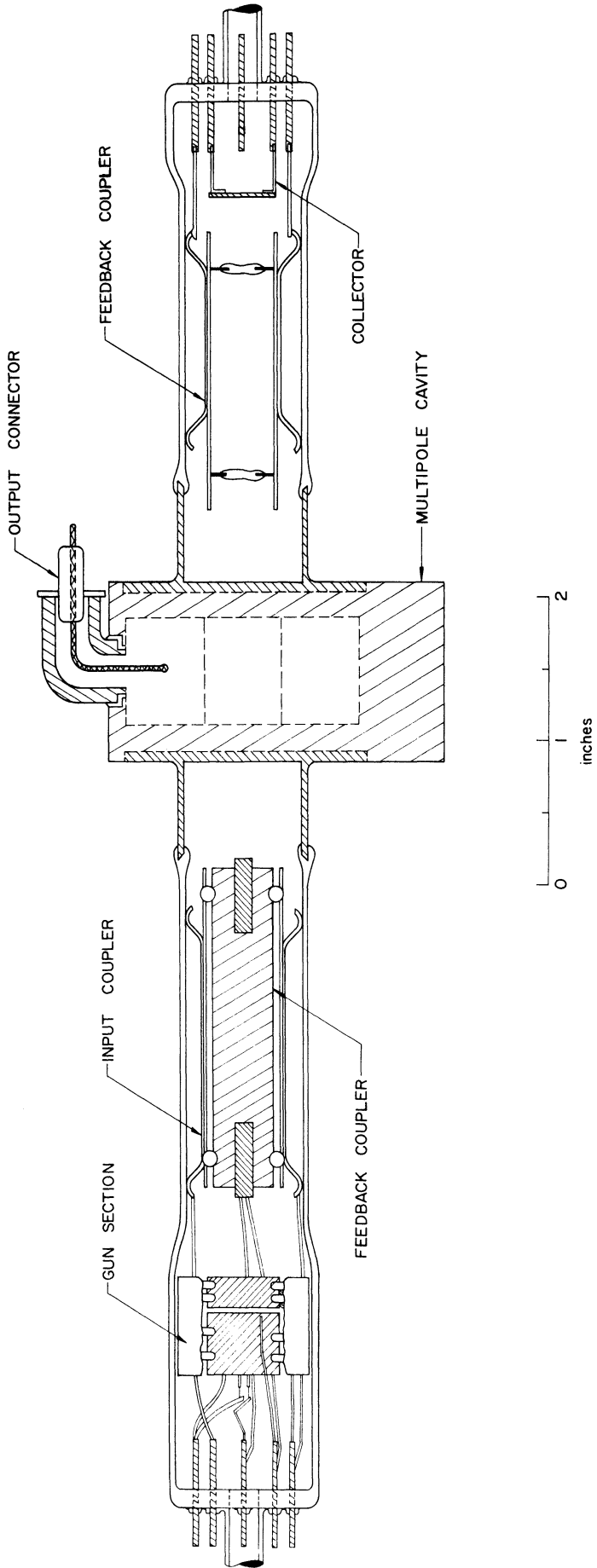


FIG. 2.1 ASSEMBLY DRAWING OF CYCLOTRON-FREQUENCY MULTIPLIER.

2.2.1a The Electron Gun. The electron gun used in this design is a conventional cathode ray gun with the second anode section removed. Since it is to be used as a low voltage gun, it may be necessary to apply a slightly positive potential to the control grid in order to get sufficient emission from the gun. The remaining parts of the tube, i.e., the coupler plates, the cavity, the feedback plates and the collector, will all be connected to the same d-c potential as the first anode. The focusing of the beam is helped by the magnetic field.

2.2.1b The Input Coupler. The input coupler consists of two pairs of mutually perpendicular Cuccia couplers. They are all connected to the same d-c potential as the first anode of the gun, but are excited, r-f wise, from two separate sources. This scheme can be achieved by a network of r-f chokes and d-c blocking capacitors, which is not shown in the assembly drawing. The plates are held together by ceramic insulators and fit into the glass wall by finger springs. The centers of the coupler are carefully aligned with the gun on one end and the cavity on the other end. One r-f source, the lower frequency input source, is connected to one pair of the couplers while the feedback source is connected to the perpendicular pair. The leads are brought out through the pins on the base.

2.2.1c The Multiplier Cavity. The multiplier cavity is adapted from a hole-slot-type cavity of an S-band magnetron. The cathode of the magnetron is removed to make room for the whirling cyclotron wave beam. The magnetic pole pieces are replaced by metal rings which extend on both sides to make connections for the couplers and the rest of the tube. The cavity has a resonant frequency of

2785 mc/s. It has a total of $N = 8$ holes. The tips of the slots are strapped so that the desired Π -mode is well separated from other modes. The output, at frequency $(N/2) \omega_c$ is taken from the cavity by a coupling loop located in one of the holes. The output connector is modified from the original design by bending it toward the cavity so that the entire structure may be inserted in a long magnetic coil three inches in diameter.

The cavity will again be biased at the same d-c potential as the first anode of the gun.

2.2.1d The Feedback Coupler. The feedback coupler consists of a single pair of plates of similar design to that of the input coupler but modified in dimensions. The leads for these plates feed through the pins on the collector side of the tube. This facilitates making the feedback connections with the input coupler outside of the tube with any desirable amount of delay inserted. The d-c potential on the plates is again the same as that on the first anode of the electron gun.

2.2.1e The Collector. The collector is simply a flat metal disc. It is maintained at the same d-c potential as the anode. Since the electron energy will be low, no special problems arise in the design of the collector.

2.2.2 Future Work. It is expected that the final assembly of the tube will be completed during the next period. Experiments with the tube can begin immediately.

2.3 Investigation of High-Thermal-Conductivity Materials for Microwave Devices Above X-Band (H. K. Detweiler)

2.3.1 Introduction. Further efforts have been made during this period to develop a satisfactory technique for brazing a tungsten

helix designed for operation at 30 Gc into a smooth-bore BeO tube.

The present effort has been directed toward finding a means for loading the helix into the tube in such a way as to obtain uniform contact. A detailed account of the work performed is given below.

2.3.2 Experimental Effort. At the conclusion of the previous quarter a procedure for preparing the helix for brazing and a satisfactory brazing cycle had been established. However, a serious difficulty had been encountered when attempts were made to load the helix into the tube. The loading technique was to first wind the helix on a mandrel so that the helix outside diameter exceeded the inside diameter of the tube by about 2 mils. After firing the helix to set it, it was wound on a smaller size mandrel so that its O.D. was about 2 to 2-1/2 mils smaller than the tube I.D. This amount of clearance was necessary so that the titanium coating on the helix would not be rubbed off during loading. It was then inserted in the tube and released. When this was done it was found that the helix did not spring back enough to make good contact with the tube. A program was undertaken to determine the firing cycle which would give the desired amount of spring to the helix in order to ensure good contact.

The first series of tests involved firing the helices in a hydrogen atmosphere at 1050°C for periods of time ranging from 25 minutes to 1-1/2 hours. In each case the helices were found to have insufficient spring-back; the helices increased on the average only 1-1/2 mils in diameter when released, whereas at least 2-1/2 mils is required.

In the next series of tests the helices were fired for long periods of time, i.e., 1 to 1-1/2 hours, in hydrogen at lower temperatures and allowing them to cool with the furnace. Again the helices failed to spring back a sufficient amount.

Next, vacuum firing of the helices was attempted. When fired at temperatures between 800°C and 1000°C for 15 minutes they were brittle and broke during attempts to wind them on the smaller diameter mandrel. When fired at temperatures below 800°C the helices did not break but as before they did not spring back enough when released.

The most recent test consisted of firing in hydrogen at 1150°C for 20 minutes. Of three helices fired in this manner, one broke when being wound down and the other two did not spring back enough when released.

It can be seen from the outcome of the above tests that the loading difficulty has not been resolved. The results of these tests seem to indicate that, when the point is reached where the helices are no longer so brittle that they break when being wound down, they do not possess sufficient resiliency to spring back more than about 1-1/2 mils. At this time, this particular approach to the problem does not seem to offer much hope of success.

2.3.3 Future Work. Work will be continued to develop a helix loading technique. An investigation will be made into the possibility of finding another suitable helix material which has a higher resiliency than tungsten. Attempts will also be made to obtain BeO tubing with greater dimensional uniformity so that less clearance between the helix and tube is required for loading. Pending successful solution of the loading problem, d-c heat tests of the power handling capability and r-f cold tests of the electrical characteristics of the brazed-helix structure will be conducted.

3. Analysis of Amplitude and Phase-Modulated Traveling-Wave Amplifiers

(M. E. El-Shandwily, J. E. Rowe)

3.1 Introduction. In the previous quarterly progress reports, an analysis was made of the operation of the TWA with a multi-frequency input. In this report, the problem is treated by another method. The reason is that the previous analysis was based on Pierce's¹ theory in which it was assumed that at any plane $z = \text{constant}$ the electron velocity is a single-valued function. Even if the initial thermal velocity spread is neglected, the crossing of the electrons when the beam is bunched makes that assumption invalid.

In order to account for electron crossovers (multivalued velocity function), the kinematics of the electron beam will be described by the Boltzmann transport equation².

This approach has been applied by Watkins and Rynn³ to study the effect of the initial velocity distribution on TWT gain, by Kiel and Parzen⁴ to study the nonlinear interaction in the TWT and by others to study the noise propagation on electron beams.

3.2 Method of Analysis. To reduce the calculations to a reasonable amount the following assumptions are made:

1. The gain parameter C is small compared to unity.
2. The tube is long enough so that at the output only the

largest growing wave is considered.

-
1. Pierce, J. R., Traveling Wave Tubes, D. Van Nostrand Co., New York, N. Y.; 1950.
 2. Rose, D. J. and Clark, Jr., M., Plasma and Controlled Fusion, M. I. T. and Wiley, N. Y., p. 58, 1961.
 3. Watkins, D. A. and Rynn, N., "Effect of Velocity Distribution on TWT Gain", Jour. Appl. Phys., vol. 25, pp. 1375-1379; November, 1954.
 4. Kiel, A. and Parzen, P., "Nonlinear Wave Propagation in TWA", IRE Trans. PGED, vol. ED-2, pp. 26-34; October, 1955.

3. There are no space-charge forces ($QC = 0$).
4. There is no loss.
5. The collision between electrons and gas molecules is neglected.
6. One-dimensional analysis.

The circuit model used is that of Brillouin⁵, and the electronic equations are replaced by the Boltzmann transport equation. Therefore the two working equations can be written as follows:

The circuit equation is

$$\frac{\partial^2 V(z,t)}{\partial t^2} - v^2 \frac{\partial^2 V(z,t)}{\partial z^2} = Z_0 v_0 \frac{\partial^2 \rho(z,t)}{\partial t^2} \quad (3.1)$$

and the Boltzmann equation is

$$\frac{\partial F(z,u,t)}{\partial t} + u \frac{\partial F(z,u,t)}{\partial z} + \eta \frac{\partial V(z,t)}{\partial z} \frac{\partial F(z,u,t)}{\partial u} = 0, \quad (3.2)$$

where ρ is the beam charge density and is given by

$$\rho = - \int_{-\infty}^{\infty} F(z,u,t) du \quad (3.3)$$

$V(z,t)$ is the circuit voltage,

v_0 is the phase velocity of the circuit voltage,

Z_0 is the circuit impedance,

$F(z,u,t)$ is the density function which gives e times the number of electrons between $z, z + dz$ with velocity between $u, u + du$ per unit beam cross section,

$\eta = |e|/m$, the magnitude of the charge-to-mass ratio of the electron.

5. Brillouin, L., "The Traveling Wave Tube", Jour. Appl. Phys., vol. 20, pp. 1196-1206; December, 1949.

To solve Eqs. 3.1 and 3.2, the boundary conditions must be specified. In this analysis it will be assumed that the input consists of two signals with angular frequencies ω_1, ω_2 .

$$\begin{aligned}
 V(0,t) &= B_1 \cos \omega_1 t + B_2 \cos \omega_2 t \\
 &= \frac{1}{2} B_1 \left(e^{j\omega_1 t} + e^{-j\omega_1 t} \right) + \frac{1}{2} B_2 \left(e^{j\omega_2 t} + e^{-j\omega_2 t} \right) . \quad (3.4a)
 \end{aligned}$$

The voltage should behave initially as

$$B_1 e^{-\alpha_1 z} \cos(\omega_1 t - \beta_1 z) + B_2 e^{-\alpha_2 z} \cos(\omega_2 t - \beta_2 z) ,$$

where $\beta_1 = \omega_1 / v_1$, $\beta_2 = \omega_2 / v_2$. Assuming that $\alpha_1 \ll \beta_1$, $\alpha_2 \ll \beta_2$, gives the following for $\partial V(z,t)/\partial z$:

$$\begin{aligned}
 \left. \frac{\partial V(z,t)}{\partial z} \right|_{z=0} &= \beta_1 B_1 \sin \omega_1 t + \beta_2 B_2 \sin \omega_2 t \\
 &= -\frac{j}{2} \beta_1 B_1 \left(e^{j\omega_1 t} - e^{-j\omega_1 t} \right) - \frac{j}{2} \beta_2 B_2 \left(e^{j\omega_2 t} - e^{-j\omega_2 t} \right) . \quad (3.4b)
 \end{aligned}$$

At the input to the tube, the beam is assumed to be unmodulated and neglecting the thermal velocity the density function becomes

$$F(0,u,t) = a \delta(u-u_0) , \quad (3.4c)$$

where $u_0^2 = 2e/m V_0$, V_0 is the d-c beam voltage and $\delta(u)$ is the Dirac delta function.

Also,

$$F(z,u,t) \rightarrow 0 \text{ as } u \rightarrow 0, u \rightarrow \infty . \quad (3.4d)$$

The problem is to solve Eqs. 3.1 and 3.2 subject to the boundary conditions (Eqs. 3.4). It is to be noted that although the circuit equation (Eq. 3.1) is linear, the Boltzmann equation is not. Therefore, the density function and the circuit voltage will contain, in addition to the input frequencies and their harmonics, all possible combinations of frequencies.

The circuit voltage and the density function will be written in the following general forms:

$$V(z,t) = \sum_{s,w=0}^{\infty} \sum_{n=-s}^s \sum_{m=-w}^w B_1^s B_2^w V_{n,m}^{(s,w)} e^{j(n\omega_1 + m\omega_2)t}, \quad (3.5)$$

$$F(z,u,t) = \sum_{s,w=0}^{\infty} \sum_{n=-s}^s \sum_{m=-s}^w B_1^s B_2^w F_{n,m}^{(s,w)} e^{j(n\omega_1 + m\omega_2)t}, \quad (3.6)$$

where $V_{n,m}^{(s,w)}$ is a function of z and $F_{n,m}^{(s,w)}$ is a function of u and z .

The expansion in the input voltages B_1 and B_2 is valid provided that these quantities are small, which is usually assumed in solving nonlinear differential equations⁶. The harmonic expansion in the input frequencies is stopped at $|n| = s$, $|m| = w$, since there can be no harmonics higher than the nonlinearity. Also, since the voltage should behave initially as $B_1 e^{j\omega_1 t} + B_2 e^{j\omega_2 t}$, then $n + s$ and $m + w$ must be even.

Equation 3.1 was derived originally for a single driving frequency. This is done by replacing the helix by an equivalent transmission line with current injected along its length. Since the equation is linear, then for every charge density component on the beam there will be

6. Minorsky, N., Non-Linear Mechanics, Edwards Brothers, Inc., Ann Arbor, Mich.; 1947.

a circuit voltage of the same frequency. Therefore Eq. 3.1 is valid for the general case of a multi-frequency input, where the circuit voltage has the general form of Eq. 3.5. Equation 3.2 is valid for any distribution function. Substituting Eqs. 3.5 and 3.6 into Eq. 3.1 gives:

$$\begin{aligned}
 & \sum_{s,w=0}^{\infty} \sum_{n=-s}^s \sum_{m=-w}^w (\nu\omega_1 + m\omega_2)^2 B_1^s B_2^w V_{n,m}^{(s,w)} e^{j(\nu\omega_1 + m\omega_2)t} \\
 & + \sum_{s,w=0}^{\infty} \sum_{n=-s}^s \sum_{m=-w}^w v_{n,m}^2 B_1^s B_2^w \frac{d^2 V_{n,m}^{(s,w)}}{dz^2} e^{j(\nu\omega_1 + m\omega_2)t} \\
 & = - \sum_{s,w=0}^{\infty} \sum_{n=-s}^s \sum_{m=-w}^w Z_{nm} v_{nm} (\nu\omega_1 + m\omega_2)^2 B_1^s B_2^w \int_0^{\infty} F_{n,m}^{(s,w)} du \\
 & \cdot e^{j(\nu\omega_1 + m\omega_2)t}, \quad (3.7)
 \end{aligned}$$

where $v_{n,m}$ is the phase velocity at frequency $|\nu\omega_1 + m\omega_2|$ and $Z_{n,m}$ is the circuit impedance at frequency $|\nu\omega_1 + m\omega_2|$.

Equating powers of $B_1^s B_2^w$ on both sides, and noting that the exponentials are orthogonal functions, then one can equate the coefficient of the exponential term on each side of Eq. 3.7 to get

$$\begin{aligned}
 (\nu\omega_1 + m\omega_2)^2 V_{n,m}^{(s,w)} + v_{n,m}^2 \frac{d^2 V_{n,m}^{(s,w)}}{dz^2} \\
 = - Z_{nm} v_{nm} (\nu\omega_1 + m\omega_2)^2 \int_0^{\infty} F_{n,m}^{(s,w)} du \quad (3.8)
 \end{aligned}$$

Substituting Eqs. 3.5 and 3.6 into Eq. 3.2 yields

$$\begin{aligned}
& \sum_{s,w=0}^{\infty} \sum_{n=-s}^s \sum_{m=-w}^w j(n\omega_1 + m\omega_2) B_1^s B_2^w F_{n,m}^{(s,w)} e^{j(n\omega_1 + m\omega_2)t} \\
& + u \sum_{s,w=0}^{\infty} \sum_{n=-s}^s \sum_{m=-w}^w B_1^s B_2^w \frac{\partial F_{n,m}^{(s,w)}}{\partial z} e^{j(n\omega_1 + m\omega_2)t} \\
& = -\eta \left(\sum_{s,w=0}^{\infty} \sum_{n''=-s}^s \sum_{m''=-w}^w B_1^s B_2^w \frac{dV_{n'',m''}^{(s,w)}}{dz} e^{j(n''\omega_1 + m''\omega_2)t} \right) \\
& \cdot \left(\sum_{s,w=0}^{\infty} \sum_{n'=-s}^s \sum_{m'=-w}^w B_1^s B_2^w \frac{\partial F_{n',m'}^{(s,w)}}{\partial u} e^{j(n'\omega_1 + m'\omega_2)t} \right).
\end{aligned}$$

Using the Cauchy product, and letting $m''+m = m$, $n'' + n = n$, the right-hand side of the above equation can be written as

$$\begin{aligned}
& \eta \sum_{s,w=0}^{\infty} \sum_{\eta=0}^s \sum_{\xi=0}^w \sum_{n=n'-\eta}^{n=n'+\eta} \sum_{m=m'-\xi}^{m'+\xi} \sum_{n'=-s+\eta}^{s-\eta} \sum_{m'=-w+\xi}^{w-\xi} B_1^s B_2^w \\
& \cdot \frac{\partial V_{n-n',m-m'}^{(\eta,\xi)}}{\partial z} \frac{\partial F_{n',m'}^{(s-\eta,w-\xi)}}{\partial u} \cdot e^{j(n\omega_1 + m\omega_2)t}.
\end{aligned}$$

The index of summation can be arranged such that the following holds:

$$\begin{aligned}
& \sum_{s,w=0}^{\infty} \sum_{n=-s}^s \sum_{m=-w}^w j(n\omega_1 + m\omega_2) B_1^s B_2^w F_{n,m}^{(s,w)} e^{j(n\omega_1 + m\omega_2)t} \\
& + u \sum_{s,w=0}^{\infty} \sum_{n=-s}^s \sum_{m=-w}^w B_1^s B_2^w \frac{\partial F_{n,m}^{(s,w)}}{\partial z} e^{j(n\omega_1 + m\omega_2)t} \\
& = -\eta \sum_{s,w=0}^{\infty} \sum_{n=-s}^s \sum_{m=-w}^w \left(\sum_{\eta=0}^s \sum_{\xi=0}^w \sum_{n'=-s}^s \sum_{m'=-w}^w B_1^s B_2^w \right. \\
& \left. \cdot \frac{\partial V_{n-n',m-m'}^{(\eta,\xi)}}{\partial z} \frac{\partial F_{n,m}^{(s-\eta,w-\xi)}}{\partial z} \right) e^{j(n\omega_1 + m\omega_2)t}.
\end{aligned}$$

Equating the coefficient of the exponential in the above equation gives

$$\begin{aligned}
 & j(n\omega_1 + m\omega_2) F_{n,m}^{(s,w)} + \frac{\partial F_{n,m}^{(s,w)}}{\partial z} \\
 &= -\eta \sum_{\eta=0}^s \sum_{\xi=0}^w \sum_{n'=-s}^s \sum_{m'=-w}^w \cdot \frac{\partial V_{n-n',m-m'}^{(\eta,\xi)}}{\partial z} \frac{\partial F_{n',m'}^{(s-\eta,w-\xi)}}{\partial u} \quad (3.9)
 \end{aligned}$$

It is found that it is more convenient to write $V(z)$, $F(z,u)$ in terms of the slowly varying variable $\Phi = \beta C z$.

$$\begin{aligned}
 V_{n,m}^{(s,w)}(z) &\equiv V'_{n,m}^{(s,w)}(\Phi_1) e^{-j \frac{\Phi_{nm}}{c_{nm}}}, \\
 F_{n,m}^{(s,w)}(z,u) &\equiv F'_{n,m}^{(s,w)}(\Phi_1, u) e^{-j \frac{\Phi_{nm}}{c_{nm}}}, \quad (3.10)
 \end{aligned}$$

where $\Phi_1 \equiv \beta_{e_1} C_1 z$ and $\beta_{e_1} = \omega_1 / u_0$.

The introduction of these variables will reduce the amount of algebra and facilitate the subsequent calculations considerably. Using Eq. 3.10, Eqs. 3.8 and 3.9 reduce to

$$\begin{aligned}
 & (n\omega_1 + m\omega_2)^2 V'_{n,m}^{(s,w)}(\Phi) + v_{nm}^2 \left[\beta^2 C^2 \frac{d^2 V'_{n,m}^{(s,w)}}{d\Phi^2} - 2 j\beta C \beta_{nm} \frac{dV'_{n,m}^{(s,w)}}{d\Phi} \right. \\
 & \left. - \beta_{nm}^2 V'_{n,m}^{(s,w)} \right] = -Z_{nm} v_{nm} (n\omega_1 + m\omega_2)^2 \int_0^\infty F'_{n,m}^{(s,w)}(\Phi, u) du \quad (3.11)
 \end{aligned}$$

and

$$\begin{aligned}
 & j (\underbrace{n\omega}_1 + \underbrace{m\omega}_2) F'_{n,m}{}^{(s,w)}(\Phi, u) + u \left[\beta C \frac{\partial F'_{n,m}{}^{(s,w)}}{\partial \Phi} - j \beta_{nm} F'_{n,m}{}^{(s,w)}(\Phi, u) \right] \\
 & = - \eta \sum_{\eta=0}^s \sum_{\xi=0}^w \sum_{n'=-s}^s \sum_{m'=-w}^w \beta C \frac{dV'_{n-n',m-m'}{}^{(\eta,\xi)}}{d\Phi} \\
 & \quad - j \beta_{n-n',m-m'} V'_{n-n',m-m'}{}^{(\eta,\xi)} \left] \frac{\partial F'_{n',m'}{}^{(s-\eta,w-\xi)}}{\partial u} \quad . \quad (3.12)
 \end{aligned}$$

A convenient way to solve the above two equations is to use the Laplace transform⁷ as given in the following definition:

$$L \left[V'_{n,m}{}^{(\eta,\xi)}(\Phi) \right] \equiv \int_0^\infty V'_{n,m}{}^{(\eta,\xi)}(\Phi) e^{-\delta\Phi} d\Phi \equiv \bar{V}'_{n,m}{}^{(\eta,\xi)}(\delta), \text{Re}(\delta) > \sigma_1, \quad (3.13a)$$

$$\begin{aligned}
 LL \left[F'_{n,m}{}^{(\eta,\xi)}(\Phi, u) \right] & \equiv \int_0^\infty \int_0^\infty F'_{n,m}{}^{(\eta,\xi)}(\Phi, u) e^{-(\delta\Phi + pu)} d\Phi du \\
 & \equiv \bar{\bar{F}}'_{n,m}{}^{(\eta,\xi)}(\delta, p), \text{Re}(\delta) > \sigma_2, \quad (3.13b)
 \end{aligned}$$

where σ_1, σ_2 are some constants which make the integration in Eqs. 3.13a and 3.13b converge.

Taking the Laplace transform of Eq. 3.11 and using the boundary conditions gives

7. Churchill, R.V., Operational Mathematics, McGraw-Hill, New York; 1958.

$$\begin{aligned}
 & (n\omega_1 + m\omega_2)^2 \bar{v}_{n,m}^{(s,w)}(\delta) + v_{nm}^2 \beta^2 c^2 \left[\delta^2 \bar{v}_{n,m}^{(s,w)}(\delta) - \delta \frac{1}{2} \delta(s,1) \delta(w,0) \right. \\
 & - \delta \frac{1}{2} (s,0) \delta(w,1) \pm j b_{1,0} c_{1,0} \frac{1}{2} \delta(s,1) \delta(w,0) \\
 & \left. \pm j b_{01} c_{01} \frac{1}{2} \delta(w,1) \delta(s,0) \right] - v_{nm}^2 \beta c \beta_{nm} \left[\delta \bar{v}_{n,m}^{(s,w)}(\delta) \right. \\
 & \left. - \frac{1}{2} \delta(s,1) \delta(w,0) - \frac{1}{2} \delta(s,0) \delta(w,1) \right] - v_{nm}^2 \beta_{nm}^2 \bar{v}_{n,m}^{(s,w)}(\delta) \\
 & = - \sum_{nm} v_{nm} (n\omega_1 + m\omega_2)^2 \bar{F}_{n,m}^{(s,w)}(\delta, 0) . \tag{3.14}
 \end{aligned}$$

The positive sign is for $n = 1$, while the negative sign is for $n = -1$.

Taking the double Laplace transform of Eq. 3.12 and using the boundary conditions yields

$$\begin{aligned}
 & j(n\omega_1 + m\omega_2) \bar{F}_{n,m}^{(s,w)}(\delta, p) + \beta c \left(- \delta \frac{\partial \bar{F}_{n,m}^{(s,w)}(\delta, p)}{\partial p} \right. \\
 & \left. - a u_0 e^{-u_0 p} \delta(s,0) \delta(w,0) + j \beta_{nm} \frac{\partial \bar{F}_{n,m}^{(s,w)}(\delta, p)}{\partial p} \right) \\
 & = - \frac{\eta p}{2\pi j} \int_{c-j\infty}^{c+j\infty} \sum_{\eta=0}^s \sum_{\xi=0}^w \sum_{n'=-s}^s \sum_{m'=-w}^w \left[\beta c \cdot (\delta-r) \bar{v}_{n-n', m-m'}^{(\eta, \xi)}(\delta-r) \right. \\
 & \left. - \frac{1}{2} \delta(s,1) \delta(w,0) \beta c - \frac{1}{2} \delta(s,0) \delta(w,1) \beta c \right. \\
 & \left. - j \beta_{n-n', m-m'} \bar{v}_{n-n', m-m'}^{(\eta, \xi)}(\delta-r) \right] \cdot \bar{F}_{n', m'}^{(s-\eta, w-\xi)}(r, p) dr , \tag{3.15}
 \end{aligned}$$

$$\begin{aligned}
 \text{where } \sigma &\equiv \text{Re}(\delta), \\
 \delta(n,m) &= 0, n \neq m \\
 &= 1, n = m \\
 C &\equiv \text{Re}(r), \\
 \sigma_1 &< C < \sigma_2.
 \end{aligned}$$

In writing Eq. 3.15 the complex convolution formula has been used to write the right-hand side⁸. The condition on the real part of r in Eq. 3.15 defines a strip in the r plane for the integration of the right-hand side. Only the poles of $\bar{F}(r,p)$ will contribute in evaluating the integral. This is because the path of integration always lies to the right of the poles of $\bar{F}(r,p)$ and to the left of the poles of the bracketed term. Therefore, by closing the contour to the left, the value of the integral over the semi-circle will vanish if $\bar{F}(r,p)$ and the bracketed term are proper rational fractions (which will be assumed), and the integral gives

$$\begin{aligned}
 2\pi j \sum \text{residue of } &\left[\left\{ \beta C(\delta-r) - j \beta_{n-n',m-m'} \right\} \bar{V}_{n-n',m-m'}^{(\eta,\xi)}(\delta-r) - \frac{1}{2} \delta(s,1)\delta(w,0)\beta C \right. \\
 &\left. - \frac{1}{2} \delta(s,0)\delta(w,1)\beta C \right] \bar{F}_{n',m'}^{(s-\eta,w-\xi)}(r,p) \text{ at the poles of } \bar{F}_{n',m'}^{(s-\eta,w-\xi)}(r,p)
 \end{aligned}$$

Rearrange the terms in Eqs. 3.14 and 3.15 and rewrite in the following final form:

8. Aseltine, J. A., Transform Method in Linear System Analysis, App. A-7, McGraw-Hill, New York; 1958.

$$\begin{aligned}
 & \bar{V}_{n,m}^{(s,w)}(\delta) \left[(n\omega_1 + m\omega_2)^2 + v_{nm}^2 (\beta^2 c^2 \delta^2 - 2j \beta c \beta_{nm} \delta - \beta_{nm}^2) \right] \\
 & + \frac{1}{2} v_{nm}^2 \left[(-\delta \pm j b_{10} c_{10}) \beta^2 c^2 + 2j \beta c \beta_{nm} \right] \delta(s,1) \delta(w,0) \\
 & + \frac{1}{2} v_{nm}^2 \left[-\delta \pm j b_{01} c_{01} \beta^2 c^2 + 2j \beta c \beta_{nm} \right] \\
 & = -Z_{nm} v_{nm} (n\omega_1 + m\omega_2)^2 \bar{F}_{n,m}^{(s,w)}(\delta,0) \quad (3.16)
 \end{aligned}$$

and

$$\begin{aligned}
 & \frac{\partial \bar{F}_{n,m}^{(s,w)}(\delta,p)}{\partial p} + \frac{j(n\omega_1 + m\omega_2)}{j\beta_{nm} - \beta c \delta} \bar{F}_{n,m}^{(s,w)}(\delta,p) - \frac{\beta c a_{00} e^{-u_0 p}}{j\beta_{nm} - \beta c \delta} \delta(s,0) \delta(w,0) \\
 & = - \frac{\eta p}{j \beta_{nm} - \beta c \delta} \frac{1}{2\pi j} \int_{c-j\infty}^{c+j\infty} \sum_{\eta=0}^s \sum_{\xi=0}^w \sum_{n'=-s}^s \sum_{m'=-w}^w \\
 & \left[\left\{ \beta c (\delta-r) - j\beta_{n-n',m-m'} \right\} \bar{V}_{n-n',m-m'}^{(\eta,\xi)}(\delta-r) - \frac{1}{2} \beta c \left\{ \delta(s,1) \delta(w,0) \right. \right. \\
 & \left. \left. + \delta(s,0) \delta(w,1) \right\} \right] \bar{F}_{n',m'}^{(s-\eta,w-\xi)}(r,p) dr \quad (3.17)
 \end{aligned}$$

In the above equations βc is $\beta_{10} c_{10}$.

3.3 Solution of the Equations. The starting point in solving Eqs. 3.16 and 3.17 is to let $s = 0, w = 0$. From Eq. 3.17 one gets $\bar{F}_{0,0}^{(0,0)}(\delta,p)$. By knowing $\bar{F}_{0,0}^{(0,0)}(\delta,p)$ and putting $s = 1, w = 0$ in Eqs. 3.16 and 3.17, then

it is possible to get $\bar{F}_{1,0}^{(1,0)}(\delta,p)$ and $\bar{V}_{1,0}^{(1,0)}(\delta)$ and repeating for $s = 0$, $w = 1$ to get $\bar{F}_{0,1}^{(0,1)}(\delta,p)$ and $\bar{V}_{0,1}^{(0,1)}(\delta)$, which are the first-order approximations. From the first-order solution the second-order approximation can be obtained and the process is repeated to get higher-order approximations. This process is carried out as follows:

From Eq. 3.17 for $s = 0$, $w = 0$

$$\frac{\partial \bar{F}_{0,0}^{(0,0)}(\delta,p)}{\partial p} + \frac{au_0}{\delta} e^{-u_0 p} = 0 ;$$

therefore,

$$\bar{F}_{0,0}^{(0,0)}(\delta,p) = \frac{a}{\delta} e^{-u_0 p} . \quad (3.18)$$

First-Order Solution

Let $s = 1$, $n = +1$, $w = 0$ in Eq. 3.17

$$\frac{\partial \bar{F}_{1,0}^{(1,0)}(\delta,p)}{\partial p} + \frac{jw}{j\beta - \beta C \delta} \bar{F}_{1,0}^{(1,0)}(\delta,p) = - \frac{\eta p}{j\beta - \beta C \delta} \frac{1}{2\pi j} \int_{c-j\infty}^{c+j\infty} \left[\left\{ \beta C(\delta-r) - j\beta \right\} \bar{V}_{1,0}^{(1,0)}(\delta-r) - \frac{\beta C}{2} \right] \cdot \bar{F}_{0,0}^{(0,0)}(r,p) dr .$$

Carrying out the contour integration on the right-hand side and then solving for $\bar{F}_{1,0}^{(1,0)}(\delta,p)$ yields

$$\bar{F}_{1,0}^{(1,0)}(\delta,p) = - \frac{\eta a \left[(C_{10} \delta - j) \bar{V}_{1,0}^{(1,0)}(\delta) - \frac{C_{10}}{2} \right] [pu_0 C_{10} - j + C_{10} \delta] e^{-pu_0}}{(u_0 C_{10} \delta)^2} . \quad (3.19)$$

For $s = 1$, $w = 0$, $n = 1$, the circuit equation (Eq. 3.16) gives:

$$\begin{aligned} \bar{V}_{1,0}^{(1,0)}(\delta) [\omega_1^2 + v_{10}^2 (\beta^2 C^2 \delta^2 - 2j \beta^2 C \delta - \beta^2)] + \frac{v_{10}^2}{2} [(-\delta + jb_{10} C_{10}) \beta^2 C^2 \\ + 2j \beta^2 C] = -Z_{10} v_{10} \omega_1^2 \bar{F}_{1,0}^{(1,0)}(\delta, 0) \quad (3.20) \end{aligned}$$

Let $p = 0$ in Eq. 3.19 and then substituting into Eq. 3.20 and arranging terms one gets:

$$\begin{aligned} \bar{V}_{1,0}^{(1,0)}(\delta) = \frac{\frac{\eta a Z_{10}}{v_{10}} C_{10} \beta_{10}^2 (-j + C_{10} \delta) + C_{10}^3 \delta^2 \beta_{10}^2 [-\delta C_{10} + jb_{10} C_{10}^2 + 2j]}{2 [\beta_{10}^2 C_{10}^2 \delta^2 (2C_{10} b_{10} - 2jC_{10} \delta + C_{10}^2 b_{10}^2 + C_{10}^2 \delta^2) - \frac{Z_{10} \eta a}{v_{10}} \beta^2 (-j + C \delta)^2]} \quad (3.21) \end{aligned}$$

At this point some useful definitions will be introduced.

Pierce's gain parameter $C_{nm}^3 = Z_{nm} I_o / 4V_o$, where Z_{nm} is the circuit impedance at frequency $(n\omega_1 + m\omega_2)$. Also, from the definition of the density function it follows that

$$I_o = \int F u du = a u_o$$

Introducing this definition into the definition of $C_{n,m}$ gives

$$C_{nm}^3 = \frac{\eta a Z_{nm}}{2u_o} \quad (3.22)$$

Substituting from Eq. 3.22 into Eq. 3.21 and neglecting terms of the order of C compared to 1 yields

$$\bar{V}_{1,0}^{(1,0)}(\delta) = \frac{\delta^2}{2j [\delta^2 (-j\delta + b_{10}) + 1]} \quad (3.23)$$

It is seen that when the denominator is equated to zero, it gives the determinantal equation of the traveling-wave tube under the assumptions made.

It will be assumed that the tube is long enough such that only the wave which corresponds to the pole with the largest real positive part is present at the output.

Taking the inverse Laplace transform of Eq. 3.23 and using the definition Eq. 3.10, one finds for the first-order approximation for the voltage with frequency ω_1

$$V_{1,0}^{(1,0)}(z,t) = \frac{\delta_1^2 e^{\beta_1 C_1 \delta_1 z}}{2j(\delta_1 - \delta_2)(\delta_1 - \delta_3)} e^{j(\omega_1 t - \beta_1 z)} \quad (3.24)$$

From the original definition of the voltage it is seen that the voltage is given by $2R_e V_{1,0}^{(1,0)}(z,t)$.

Substituting Eq. 3.23 into Eq. 3.19 and making the same approximations, one gets

$$\bar{F}_{1,0}^{(1,0)}(\delta,p) = \frac{\eta a [p u_0 C_{10} \delta - j] e^{-p u_0}}{2u_0^2 C_{10}^2 [\delta^2(-j\delta + b_{10}) + 1]} \quad (3.25)$$

To obtain the first-order solution for the signal with frequency ω_2 , the above procedure is repeated for $s = 0$, $w = 1$, $m = 1$, and the result is

$$\bar{V}_{0,1}^{(0,1)}(\delta) = \frac{\frac{\beta_{10}^2 C_{10}^2}{\beta_{01}^2 C_{01}^2} \delta^2}{2j \frac{\beta_{01} C_{01}}{\beta_{10} C_{10}} \left[\frac{\beta_{10}^2 C_{10}^2}{\beta_{01}^2 C_{01}^2} \delta^2 \left(-j \frac{\beta_{10} C_{10}}{\beta_{01} C_{01}} \delta + b_{01} \right) + 1 \right]} \quad (3.26)$$

$$\bar{F}_{0,1}^{(0,1)}(\delta,p) = \frac{\eta a e^{-p u_0} \left[\frac{p u_0 \beta_{10} C_{10}}{\beta_{01} C_{01}} C_{01} \delta - j \right]}{2u_0^2 C_{01}^2 \frac{\beta_{01} C_{01}}{\beta_{10} C_{10}} \left[\frac{\beta_{10}^2 C_{10}^2}{\beta_{01}^2 C_{01}^2} \delta^2 \left(- \frac{j \beta_{10} C_{10}}{\beta_{01} C_{01}} \delta + b_{01} \right) + 1 \right]} \quad (3.27)$$

Assuming that the circuit is nondispersive in a certain frequency band and that ω_1 and ω_2 are within this band, then $b_{10} = b_{01}$. Taking the inverse Laplace transform of Eq. 3.26 one obtains

$$V_{0,1}^{(0,1)}(z,t) = \frac{\delta_1^2 e^{\beta_{01} C_{01} \delta_1 z}}{2j (\delta_1 - \delta_2) (\delta_1 - \delta_3)} e^{j(\omega_2 t - \beta_{01} z)}, \quad (3.28)$$

which, when multiplied by the input with frequency ω_2 , gives the first approximation to the circuit voltage with frequency ω_2 .

Second-Order Solution

The second-order approximation is obtained from the general Eqs. 3.16 and 3.17 by letting $s = 2, w = 0$; $s = 0, w = 2$ and $s = 1, w = 1$. Considering the case $s = 2, w = 0$, therefore $m = 0, n = 0$ or 2. For $s = 2, w = 0, m = 0, n = 0$, Eq. 3.17 gives

$$\begin{aligned} \frac{\partial \bar{F}_{0,0}^{(2,0)}(\delta,p)}{\partial p} &= \frac{\eta p}{\beta_{10} C_{10} \delta} \frac{1}{2\pi j} \int_{c-j\infty}^{c+j\infty} \left[\bar{V}_{-1,0}^{(1,0)}(\delta-r) \right. \\ &\quad \cdot \bar{F}_{1,0}^{(1,0)}(r-p) [\beta_{10} C_{10}(\delta-r) - j\beta_{-10}] + \bar{V}_{1,0}^{(1,0)}(\delta-r) \\ &\quad \left. \cdot \bar{F}_{-1,0}^{(1,0)}(r,p) [\beta_{10} C_{10}(\delta-r) - j\beta_{10}] \right] dr . \end{aligned}$$

Note that $\bar{V}_{-1,0}^{(1,0)}$ and $\bar{F}_{-1,0}^{(1,0)}$ are obtained from $\bar{V}_{1,0}^{(1,0)}$ and $\bar{F}_{1,0}^{(1,0)}$, respectively, by changing j into $(-j)$. The complex integration on the right-hand side is carried out only over the pole with the largest positive real part. Carrying out the complex integration and then integrating with respect to p , the result is:

$$\bar{F}_{0,0}^{(2,0)}(\delta,p) = \frac{\eta^2 a e^{-pu_0}}{4 j C_{10}^3 u_0^4 \delta}$$

$$\cdot \left[\frac{(\delta - \delta_1)^2 \{C_{10}(\delta - \delta_1) + j\} \{pu_0(-j + pu_0 C_{10} \delta_1) + (j + 2pu_0 C_{10} \delta_1) 2C_{10} \delta_1\}}{(\delta_1 - \delta_2)(\delta_1 - \delta_3) [(\delta - \delta_1)^2 \{j(\delta - \delta_1) + b\} + 1]} \right.$$

$$\left. - \frac{(\delta - \delta_1^*)^2 \{C_{10}(\delta - \delta_1^*) - j\} \{pu_0(j + pu_0 C_{10} \delta_1^*) + (j + 2pu_0 C_{10} \delta_1^* + 2C_{10} \delta_1^*)\}}{(\delta_1^* - \delta_2^*)(\delta_1^* - \delta_3^*) [(\delta - \delta_1^*)^2 \{-j(\delta - \delta_1^*) + b\} + 1]} \right].$$

(3.29)

For $s = 2, w = 0, m = 0, n = 2$, Eq. 3.17 gives

$$\frac{\partial \bar{F}_{2,0}^{(2,0)}(\delta,p)}{\partial p} + \frac{2j\omega_1}{j\beta_{20} - \beta_{10} C_{10} \delta} \bar{F}_{2,0}^{(2,0)}(\delta,p) = - \frac{\eta p}{j\beta_{20} - \beta_{10} C_{10} \delta} \frac{1}{2\pi j} \int_{c-j\infty}^{c+j\infty}$$

$$\cdot \left[\{\beta_{10} C_{10}(\delta-r) - j\beta_{10}\} \bar{V}_{1,0}^{(1,0)}(\delta-r) \bar{F}_{1,0}^{(1,0)}(r,p) \right.$$

$$\left. + \{\beta_{10} C_{10}(\delta-r) - j\beta_{2,0}\} \bar{V}_{2,0}^{(2,0)}(\delta-r) \bar{F}_{0,0}^{(0,0)}(\delta-r) \right] dr.$$

Carrying out the complex integration on the right-hand side as before and then integrating the resulting linear differential equation in $\bar{F}_{2,0}^{(2,0)}(\delta,p)$ gives

$$\bar{F}_{2,0}^{(2,0)}(\delta_1) = -\frac{\eta a e^{-pu_0}}{u^2 C^2 \delta_{0,10}^2} \left[- (2j - C_{10} \delta) \{ pu C_{10} \delta - 2j + C_{10} \delta \} \bar{V}_{2,0}^{(2,0)} \right]$$

$$+ \frac{\eta (\delta - \delta_1)^2 \{ C_{10} (\delta - \delta_1) - j \} \{ 2\delta_{10} (2j - C_{10} \delta)^2 - \delta (-j + 2pu C_{10} \delta) (2j - C_{10} \delta) + pu C_{10} \delta^2 (-j + pu C_{10} \delta) \}}{2j\delta (\delta - \delta_1) (\delta - \delta_2) (\delta - \delta_3) [(\delta - \delta_1)^2 \{-j(\delta - \delta_1) + b_{10}\} + 1] \cdot 2u^2 C_{10}^2} \quad (3.30)$$

From Eq. 3.16 for $s = 2$, $w = 0$, $m = 0$, $n = 2$

$$\bar{V}_{2,0}^{(2,0)}(\delta) [(2\omega_1)^2 + v_{2,0}^2 (\beta_{10}^2 C_{10}^2 \delta^2 - 2j\beta_{10} C_{10} \beta_{20} \delta - \beta_{20}^2)] = -Z_{20} v_{20} (2\omega_1)^2 F_{2,0}^{(2,0)}(\delta, 0) \quad (3.31)$$

By putting $p = 0$ in Eq. 3.30 and solving the resulting equation with Eq. 3.31 for the second harmonic voltage of the signal with frequency ω_1 , the result is:

$$\bar{V}_{2,0}^{(2,0)}(\delta) = \frac{\eta C_{10}^3 (\delta - \delta_1)^2 [C_{10} (\delta - \delta_1) - j] (2j - C_{10} \delta) [2\delta_{10} (2j - C_{10} \delta) + j\delta]}{4ju^2 C_{10}^5 (\delta - \delta_1) (\delta - \delta_2) (\delta - \delta_3) \delta [(\delta - \delta_1)^2 \{-j(\delta - \delta_1) + b_{10}\} + 1] \left[4 \left(\frac{C_{20}}{C_{10}^3} \right) + \delta^2 (-j \frac{\delta}{2} + b_{20}) \right]} \quad (3.32)$$

where the definition $2\omega_1/v_{20} = \beta_{20} (1 + C_{10} b_{10})$ has been used.

The pole with the largest positive real part of Eq. 3.32 is

$\delta = 2 \delta_1$. Therefore,

$$\begin{aligned} & \bar{V}_{2,0}^{(2,0)}(\varphi) \\ &= + \frac{3}{16} \left(\frac{C_{2,0}}{C_{1,0}} \right)^3 \frac{\delta_1^2 e^{2\beta_{10} C_{10} \delta_1} e^{2j(\omega_1 t - \beta_{10} z)}}{V_0 C_{10}^2 (\delta_1 - \delta_2)^2 (\delta_1 - \delta_3)^2 \left[\frac{C_{20}^3}{C_{10}^3} + \delta_1^2 (-j\delta_1 + b_{20}) \right]}, \end{aligned} \quad (3.33)$$

where C_{20} is the gain parameter at frequency $2\omega_1$.

If the circuit is nondispersive then b_{20} will be equal to b_{10} , and therefore $\delta_1^2 (-j\delta_1 + b_{20}) = -1$. If $(C_{20}/C_{10})^3$ can be neglected compared to unity (which is almost true, since the circuit impedance at the harmonic frequency is much smaller than its value at the fundamental), Eq. 3.33 reduces to the following expression:

$$\bar{V}_{2,0}^{(2,0)}(\varphi) = - \frac{3}{16} \left(\frac{C_{20}}{C_{10}} \right)^3 \frac{\delta_1^2 e^{2\beta_{10} C_{10} \delta_1} e^{2j(\omega_1 t - \beta_{10} z)}}{V_0 C_{10}^2 (\delta_1 - \delta_2)(\delta_1 - \delta_3)}. \quad (3.34)$$

Multiplying Eq. 3.34 by B_1^2 and taking twice the real part gives the second harmonic voltage of the signal at frequency ω_1 . It should be noted that the above expression gives the first-order approximation to the second harmonic voltage. Higher-order approximations could be obtained. However, the next order will be proportional to B_1^4 and to $B_1^2 B_2^2$. This will not be carried out here.

By the same procedure, the second harmonic voltage of the signal at ω_2 can be obtained. The result is

$$\bar{V}_{0,2}^{(0,2)}(\varphi) = -\frac{3}{16} \left(\frac{C_{02}}{C_{01}} \right)^3 \frac{\delta_1^2 e^{2\beta_{01} C_{01} \delta_1} e^{2j(\omega_2 t - \beta_{01} Z)}}{V_0 C_{01}^2 (\delta_1 - \delta_2)^2 (\delta_1 - \delta_3)^2} . \quad (3.35)$$

Third-Order Solution

The third-order approximation to the voltage at frequency ω_1 is obtained by putting $s = 3$, $w = 0$, $n = 1$ and $s = 1$, $n = 1$, $w = 2$ $m = 0$. The first case gives the dependence on B_1 as B_1^3 , whereas the second case gives dependence on B_1 and B_2 as $B_1 B_2^2$.

$$\begin{aligned} \frac{\partial \bar{F}_{1,0}^{(3,0)}(\delta, p)}{\partial p} + \frac{j\omega_1}{j\beta_1 - \beta_1 C_{10} \delta} \bar{F}_{1,0}^{(3,0)}(\delta, p) &= -\frac{\eta p}{j\beta_{10} - B_{10} C_{10} \delta} \\ &\cdot \frac{1}{2\pi j} \int_{c-j\infty}^{c+j\infty} \left[\bar{V}_{1,0}^{(1,0)}(\delta-r) \bar{F}_{0,0}^{(2,0)}(r, p) [\beta_{10} C_{10}(\delta-r) - j\beta_{10}] \right. \\ &+ \bar{V}_{-1,0}^{(1,0)}(\delta-r) \bar{F}_{2,0}^{(2,0)}(r, p) [\beta_{10} C_{10}(\delta-r) - j\beta_{-1,0}] \\ &+ \bar{V}_{2,0}^{(2,0)}(\delta-r) \bar{F}_{-1,0}^{(1,0)}(r, p) [\beta_{10} C_{10}(\delta-r) - j\beta_{2,0}] \\ &\left. + \bar{V}_{1,0}^{(3,0)}(\delta-r) \bar{F}_{0,0}^{(0,0)}(r, p) \cdot [\beta_{10} C_{10}(\delta-r) - j\beta_{10}] \right] dr . \quad (3.36) \end{aligned}$$

To facilitate the calculations, the second harmonic voltage will be neglected. Use Eqs. 3.23, 3.27, 3.29 and 3.30 and integrate over the pole with the largest positive real part, then integrating the resulting first-order equation in $\bar{F}_{1,0}^{(3,0)}(\delta, p)$, the result is

where $A = u_0 C_{10} \delta / (j - C_{10} \delta)$.

From the circuit equation (Eq. 3.16) for $s = j$, $n = 1$, $w = 0$,

$$\bar{V}_{1,0}^{(3,0)}(\delta) [\omega_1^2 + v_{10}^2 (\beta_{10}^2 C_{10}^2 \delta^2 - 2j\beta_{10}^2 C_{10} \delta - \beta_{10}^2)] = -Z_{10} v_{10} \omega_1^2 \bar{F}_{1,0}^{(3,0)}(\delta, 0) .$$

By solving Eqs. 3.37 and 3.38 for $\bar{V}_{1,0}^{(3,0)}(\delta)$, the result is (3.38)

$$\bar{V}_{(1,0)}^{(3,0)}(\delta) = \frac{(j - c_{10}\delta)}{32 \cdot c_{10}^4 \cdot v^2 \delta^2 [\delta^2(-j\delta + b_{10}) + 1]}$$

$$\cdot \frac{(\delta - \delta_1 - \delta_1^*)^2 (c_{10}(\delta - \delta_1 - \delta_1^*) - j) (\delta_1^{*2} (c_{10}\delta_1^* + j) - j) (\delta_1^{*2} (c_{10}\delta_1^* + j) + 2\delta(j - c_{10}\delta)) (c_{10}\delta_1 - j) - 6\delta_1(j - c_{10}\delta)^2 - \delta_1^2 (c_{10}\delta_1 - j) [-c_{10}\delta^2 (2c_{10}\delta_1^* + j) + 2\delta(j - c_{10}\delta)] (c_{10}\delta_1^* + j) - 6\delta_1^* (j - c_{10}\delta)^2]}{(\delta_1 - \delta_2)(\delta_1 - \delta_3)(\delta_1^* - \delta_2^*)(\delta_1^* - \delta_3^*)(\delta_1 + \delta_1^*)(\delta_1 - \delta_2^*)^2 [(j - \delta_1 - \delta_1^*)^2 + b_{10}] + 1}$$

$$+ \frac{(c_{10}\delta_1 - j)(\delta - 2\delta_1)^2 (c_{10}(\delta - 2\delta_1) + j) [-2(j - c_{10}\delta_1)(3j - c_{10}\delta_1)\delta^2 + 4\delta_1\delta(-3j + 2c_{10}\delta_1)(j - c_{10}\delta)] - 2\delta_1^2 (j - c_{10}\delta)^2}{4(\delta_1 - \delta_2)^2 (\delta_1 - \delta_3)^2 [(j - 2\delta_1)^2 + b_{10}] + 1} \tag{3.39}$$

By taking the inverse transform of Eq. 3.39, neglecting terms of order of C compared to unity and rearranging terms, the final result is:

$$V_{1,0}^{(3,0)}(z,t) = \frac{j[5\delta_1^* \delta_1^2 - 2\delta_1^3 + 3\delta_1 \delta_1^{*2} + (3/2)\delta_1^{*2}(2\delta_1 + \delta_1^*)] e^{\beta_{10} C_{10}(2\delta_1 + \delta_1^*)z} e^{j(\omega_1 t - \beta_{10} z)}}{32V_{0,10}^2 C_{10}^4 (\delta_1 - \delta_2)^2 (\delta_1 - \delta_3)^2 (\delta_1^* - \delta_2^*) (\delta_1^* - \delta_3^*) (2\delta_1 + \delta_1^*) (\delta_1 + \delta_1^*) (2\delta_1 + \delta_1^* - \delta_2) (2\delta_1 + \delta_1^* - \delta_3)} \quad (3.40)$$

Equation 3.40 does not give the total third-order approximation, it is only that part which depends on B_1^3 . The other part depends on $B_1 B_2^2$, it is $\bar{V}_{1,0}^{(1,2)}(\delta)$. This is obtained from Eqs. 3.16 and 3.17 for $s = 1, w = 2, m = 0, n = 1$. Equation 3.17 gives

$$\frac{\partial \bar{F}_{1,0}^{(1,2)}(\delta,p)}{\partial p} + \frac{j\omega_1}{j\beta_{10} - \beta_{10} C_{10} \delta} \bar{F}_{1,0}^{(1,2)}(\delta,p) = - \frac{\eta p}{j\beta_{10} - \beta_{10} C_{10} \delta} \cdot \frac{1}{2\pi j} \int_{c-j\infty}^{c+j\infty} \cdot \left[\bar{V}_{0,-1}^{(0,1)}(\delta-r) \bar{F}_{1,1}^{(1,1)}(r,p) [\beta_{10} C_{10}(\delta-r) - j\beta_{0,-1}] \right. \\ + \bar{V}_{0,1}^{(0,1)}(\delta-r) \bar{F}_{1,-1}^{(1,1)}(r,p) [\beta_{10} C_{10}(\delta-r) - j\beta_{0,1}] \\ + \bar{V}_{1,0}^{(1,0)}(\delta-r) \bar{F}_{0,0}^{(0,2)}(r,p) [\beta_{10} C_{10}(\delta-r) - j\beta_{10}] \\ + \bar{V}_{(1,-1)}^{(1,1)}(\delta-r) \bar{F}_{0,1}^{(0,1)}(r,p) [\beta_{10} C_{10}(\delta-r) - j\beta_{1,-1}] \\ + \bar{V}_{1,1}^{(1,1)}(\delta-r) \bar{F}_{0,-1}^{(0,1)}(r,p) [\beta_{10} C_{10}(\delta-r) - j\beta_{1,1}] \\ \left. + \bar{V}_{1,0}^{(1,2)}(\delta-r) \bar{F}_{0,0}^{(0,0)}(r,p) [\beta_{10} C_{10}(\delta-r) - j\beta_{10}] \right] dr \quad (3.41)$$

As before the second harmonic voltages will be neglected, also the voltages at frequencies $\omega_1 + \omega_2$ and $\omega_1 - \omega_2$ will be neglected. These are reasonable assumptions when the frequencies ω_1 and ω_2 are not very much different and both near the center of the band. It should be noted that although $\bar{V}_{1-1}^{(1,1)}(\delta)$, $\bar{V}_{1,1}^{(1,1)}(\delta)$ can be neglected but $\bar{F}_{1,-1}^{(1,1)}(\delta, p)$, $\bar{F}_{1,1}^{(1,1)}(\delta, p)$ cannot. This is because the harmonic content of the beam might be large, but its effect on the circuit is small because the impedance of the circuit at these frequencies is small.

To evaluate Eq. 3.41 one needs the following quantities in addition to those previously derived: $\bar{F}_{1,1}^{(1,1)}(\delta, p)$, $\bar{F}_{1,1}^{(1,1)}(\delta, p)$ and $\bar{F}_{0,0}^{(0,2)}(\delta, p)$. Using the same procedure as before, these are:

$$\bar{F}^{(1,1)}_{(1,-1)}(\delta, p) = - \frac{\eta^2 a e^{-pu_0}}{4jv\beta^3 C^3 \delta^3}$$

$$\left[\frac{-j\beta_{10} + \beta_{10} C_{1010} \left(\delta - \frac{\beta_{01} C_{01}}{\beta_{1010}} \delta^* \right)}{\left(\delta - \frac{\beta_{01} C_{01}}{\beta_{1010}} \delta^* \right)^2} \left[p \left(pu_{0011} C_{0011} \delta^* + j \right) u_{01010}^2 C_{01010}^2 \delta^2 - (+j+2pu_{0011} C_{0011} \delta^*) (j\beta_{1-1} - \beta_{1010} C_{1010} u_{01010} \beta_{1010} C_{1010} \delta + (j\beta_{1-1} - \beta_{1010} C_{1010})^2 2u_{0011} C_{0011} \delta^* \right) \right] \right. \\ \left. C_{0112}^2 (\delta^* - \delta^*) (\delta^* - \delta^*) \left[\left(\delta - \frac{\beta_{01} C_{01}}{\beta_{1010}} \delta^* \right)^2 \left\{ -j \left(\delta - \frac{\beta_{01} C_{01}}{\beta_{1010}} \delta^* \right) + b \right\} + 1 \right] \right]$$

$$\left[\frac{+j\beta_{01} + \beta_{01} C_{1010} (\delta - \delta)}{\beta_{01} C_{01}^2} (\delta - \delta)^2 \left\{ p \left(pu_{010} C_{010} \delta - j \right) u_{01010}^2 C_{01010}^2 \delta^2 - (-j+2pu_{0011} C_{0011} \delta) (j\beta_{1-1} - \beta_{1010} C_{1010} u_{01010} \beta_{1010} C_{1010} \delta + (j\beta_{1-1} - \beta_{1010} C_{1010})^2 2u_{0011} C_{0011} \delta) \right\} \right. \\ \left. C_{1012}^2 (\delta - \delta) (\delta - \delta) \left[\frac{C_{01} \beta_{01}}{C_{1010} \beta_{1010}} \left[\frac{\beta_{01} C_{01}}{\beta_{1010}} (\delta - \delta) + b \right] + 1 \right] \right]$$

(3.42)

$$\bar{F}_{1,1}^{(1,1)}(\delta, p) = \frac{-\eta^2 a e^{-pu_0}}{4ju_0^5 (\beta_{1010}^C)^3 (\delta_1 - \delta_2)(\delta_1 - \delta_3)\delta_3}$$

$$\left[\beta_{1010}^C \left(\delta - \frac{\beta_{0101}^C}{\beta_{1010}^C} \delta_1 \right) - j\beta_{10}^C \right] \left(\delta - \frac{\beta_{0101}^C}{\beta_{1010}^C} \delta_1 \right)^2 \left[p(pu_{0101}^C \delta_1 - j)u_{0101}^2 C^2 \delta_1^2 - (-j+2pu_{0101}^C \delta_1)(j\beta_{111010}^C \delta_1 + (j\beta_{111010}^C \delta_1)^2 2u_{0101}^C \delta_1) \right]$$

$$C_{01}^2 \left[\left(\delta - \frac{\beta_{0101}^C}{\beta_{1010}^C} \delta_1 \right)^2 \left\{ -j \left(\delta - \frac{\beta_{0101}^C}{\beta_{1010}^C} \delta_1 \right) + b_{10} \right\} + 1 \right]$$

$$\left[\beta_{1010}^C (\delta - \delta_1) - j\beta_{01}^C \right] (\delta - \delta_1)^2 \frac{\beta_{1010}^2 C^2}{\beta_{01}^2 C^2} \left[p(pu_{0101}^C \delta_1 - j)u_{0101}^2 C^2 \delta_1^2 - (-j+2pu_{0101}^C \delta_1)(j\beta_{111010}^C \delta_1 + (j\beta_{111010}^C \delta_1)^2 2u_{101}^C \delta_1) \right]$$

$$+ \frac{\beta_{0101}^C}{\beta_{1010}^C} C^2 \left\{ \frac{\beta_{1010}^2 C^2}{\beta_{01}^2 C^2} (\delta - \delta_1)^2 \left[-j \frac{\beta_{1010}^C}{\beta_{01}^C} (\delta - \delta_1) + b_{01} \right] + 1 \right\}$$

(3.43)

$$\begin{aligned}
 \bar{F}_{0,0}^{(0,2)}(\delta, p) &= \frac{\eta^2 a e^{-pu} \beta_{1010}^3 C^3}{4ju \beta_{0101010101} C^2 \beta_{01}^3 C^3} \\
 &= \frac{\left[\beta_{1010} C \left(\delta - \frac{\beta_{01} C_{01}}{\beta_{1010} C} \delta \right) + j\beta_{01} \right] \left(\delta - \frac{\beta_{01} C_{01}}{\beta_{1010} C} \delta \right)^2 \left[pu \left(-j+pu C_{01} \delta \right) + (-j+2pu C_{01} \delta) + 2C_{01} \delta \right]}{\left(\delta_{12} - \delta \right) (\delta_{12} - \delta) \left[\frac{\beta_{1010}^2 C^2}{\beta_{01}^2 C^2} \left(\delta - \frac{\beta_{01} C_{01}}{\beta_{1010} C} \delta \right)^2 \left\{ j \frac{\beta_{1010} C}{\beta_{01} C_{01}} \left(\delta - \frac{\beta_{01} C_{01}}{\beta_{1010} C} \delta \right) + b_{01} \right\} + 1 \right]} \\
 &+ \frac{\left[\beta_{1010} C \left(\delta - \frac{\beta_{01} C_{01}}{\beta_{1010} C} \delta^* \right) - j\beta_{01} \right] \left(\delta - \frac{\beta_{01} C_{01}}{\beta_{1010} C} \delta^* \right)^2 \left[pu \left(j+pu C_{01} \delta^* \right) + (j+2pu C_{01} \delta^*) + 2C_{01} \delta^* \right]}{\left(\delta_{12}^* - \delta \right) (\delta_{12}^* - \delta) \left[\left(\frac{\beta_{1010} C}{\beta_{01} C_{01}} \right)^2 \left(\delta - \frac{\beta_{01} C_{01}}{\beta_{1010} C} \delta \right) \left(\delta - \frac{\beta_{01} C_{01}}{\beta_{1010} C} \delta^* \right) + b_{01} \right] + 1}
 \end{aligned} \tag{3.44}$$

Using Eqs. 3.42, 3.43, 3.44 and the previous quantities, it is possible to evaluate the complex integration of Eq. 3.40 and then solve the resulting linear first-order differential equation in $\bar{F}_{1,0}^{(1,2)}(\delta, p)$. After obtaining $\bar{F}_{1,0}^{(1,2)}(\delta, p)$, together with $\bar{V}_{1,0}^{(1,2)}(\delta)$ (from the circuit equation), one can solve for $\bar{V}_{1,0}^{(1,2)}(\delta)$; the result after taking the inverse transform is

Multiply Eq. 3.40 by B_1 and Eq. 3.45 by $B_1 B_2^2$ and add; then take twice the real part, which gives the third-order voltage. In this analysis it will be considered sufficient to stop at the third-order approximation.

High-Order Difference Frequency Components

If the frequency difference $(\omega_1 - \omega_2)$ between the two input signals is not large, according to the general expressions, Eqs. 3.5 and 3.6, there will be components with frequencies in the passband of the circuit. Two of these components are with frequencies $2\omega_1 - \omega_2$ and $2\omega_2 - \omega_1$. The component with frequency $2\omega_1 - \omega_2$ will be derived.

Substituting $s = 2$, $n = 2$, $w = 1$, $m = -1$ in Eqs. 3.16 and 3.17 one gets:

$$\begin{aligned} \bar{V}_{2,-1}^{(2,1)}(\delta) & [(2\omega_1 - \omega_2)^2 + v_{2,-1}^2 (\beta_{10}^2 C_{10}^2 \delta^2 - 2j\beta_{10} C_{10} \beta_{2,-1} \delta - \beta_{2,-1}^2)] \\ & = - Z_{2,-1} v_{2,-1} (2\omega_1 - \omega_2)^2 \bar{F}_{2,-1}^{(2,1)}(\delta, 0) \quad , \quad (3.46) \end{aligned}$$

$$\begin{aligned} & \frac{\partial \bar{F}_{2,-1}^{(2,1)}(\delta, p)}{\partial p} + \frac{j(2\omega_1 - \omega_2)}{j(2\beta_{10} - \beta_{01}) - \beta_{10} C_{10} \delta} \bar{F}_{2,-1}^{(2,1)}(\delta, p) \\ & = - \frac{\eta p}{j(2\beta_{10} - \beta_{01}) - \beta_{10} C_{10} \delta} \cdot \frac{1}{2\pi j} \int_{c-j\infty}^{c+j\infty} \left[\bar{V}_{2,-1}^{(2,1)}(\delta-r) \bar{F}_{0,0}^{(0,0)}(r, p) \right. \\ & \quad \cdot \{ \beta_{10} C_{10} (\delta-r) - j\beta_{10} \} + \bar{V}_{1,0}^{(1,0)}(\delta-r) \bar{F}_{1,-1}^{(1,1)}(r, p) \\ & \quad \left. \cdot \{ \beta_{10} C_{10} (\delta-r) - j\beta_{10} \} + \bar{V}_{0,-1}^{(0,1)}(\delta-r) \bar{F}_{(2,0)}^{(2,0)}(r, p) \{ \beta_{10} C_{10} (\delta-r) - j\beta_{0,-1} \} \right] dr \quad . \end{aligned} \quad (3.47)$$

Integrate the right-hand side and then solve the linear first-order equation in $\bar{F}_{2,-1}^{(2,1)}(\delta, p)$. The solution of Eq. 3.47 for $\bar{F}_{2,-1}^{(2,1)}(\delta, p)$ is solved simultaneously with Eq. 3.46 for $\bar{V}_{2,-1}^{(2,1)}(\delta)$, and the result after taking the inverse Laplace transform is:

The circuit voltage at $2\omega_2 - \omega_1$ can be obtained from Eq. 3.48 by interchanging 1 and 0.

It should be noted that the circuit voltage is obtained from Eq. 3.48 by multiplying the right-hand side by $B_1^2 B_2$ and taking twice the real part.

Other intermodulation components can be obtained in the same way.

3.4 Program for the Next Quarter. The equations presented in the first quarterly progress report are being programmed for digital computer solution. The results will be presented in the form of curves representing different operating conditions. Also, it is intended to program the equations of the second progress report.

No experimental work has been done during this period. However, it is planned to initiate experimental studies on an X-band TWA during the next period.

4. Study of a D-c Pumped Quadrupole Amplifier (C. Yeh, B. Ho)

4.1 Introduction. In Quarterly Progress Report No. 2, the state-of-the-art of cyclotron-wave devices was reviewed. It was suggested then that a unified analysis should be carried out so that the coupling mechanism among different modes of operation could be better understood, and a fair comparison between the different coupling mechanisms could be made. To achieve these objectives, an analysis based upon coupled-mode theory was carried out during this reporting period. Although the coupled-mode method does not represent an accurate picture of this device, especially for large-signal operation, the simple mathematics it uses enables one to visualize the physical insight of the device and, in particular, the interaction mechanism between the different modes of coupling.

4.2 Coupled-Mode Equations of Beam Dynamics. Consider a filamentary electron beam in spatially varying electric and magnetic fields, the transverse equations of motion in rectangular coordinates are

$$\frac{d}{dt} v_x = -\eta (E_x + v_y B_z - v_z B_y) \quad (4.1)$$

and

$$\frac{d}{dt} v_y = -\eta (E_y - v_x B_z + v_z B_x) \quad , \quad (4.2)$$

where η is the charge-to-mass ratio. The transverse displacements and transverse velocities are related by

$$\frac{dx}{dt} = v_x \quad (4.3)$$

and

$$\frac{dy}{dt} = v_y \quad . \quad (4.4)$$

With a static axial magnetic field $B_z = B_0$, and assume constant $v_z = u_0$, Eqs. 4.1-4.4 can be put into a set of coupled-mode equations in terms of mode amplitudes as follows:

$$\left(\frac{d}{dt} - j\omega_c\right) a_1 = -\eta k(E_+ + ju_0 B_+) + \frac{1}{k} \frac{dk}{dt} a_1 \quad , \quad (4.5)$$

$$\left(\frac{d}{dt} + j\omega_c\right) a_2 = -\eta k(E_- - ju_0 B_-) + \frac{1}{k} \frac{dk}{dt} a_2 \quad , \quad (4.6)$$

$$\frac{da_3}{dt} = -\eta k(E_+ + ju_0 B_+) + \frac{1}{k} \frac{dk}{dt} a_3 + \frac{1}{\omega_c} \frac{d\omega_c}{dt} (a_3 - a_1) \quad , \quad (4.7)$$

$$\frac{da_4}{dt} = -\eta k(E_- - ju_0 B_-) + \frac{1}{k} \frac{dk}{dt} a_4 + \frac{1}{\omega_c} \frac{d\omega_c}{dt} (a_4 - a_2) \quad , \quad (4.8)$$

where

$$\begin{aligned}
 a_1 &= \text{fast cyclotron wave} \\
 &= A_1 e^{-j(\beta_e - \beta_c)z} \\
 &= k(v_x + j v_y) \quad , \quad (4.9)
 \end{aligned}$$

$$\begin{aligned}
 a_2 &= \text{slow cyclotron wave} \\
 &= A_2 e^{-j(\beta_e + \beta_c)z} \\
 &= k(v_x - j v_y) \quad , \quad (4.10)
 \end{aligned}$$

$$\begin{aligned}
 a_3 &= \text{negative (kinetic power)} \\
 &\quad \text{synchronous wave} \\
 &= A_3 e^{-\beta_e z} \\
 &= k[v_x + j v_y - j\omega_c(x + jy)] \quad , \quad (4.11)
 \end{aligned}$$

$$\begin{aligned}
 a_4 &= \text{positive (kinetic power)} \\
 &\quad \text{synchronous wave} \\
 &= A_4 e^{-j\beta_e z} \\
 &= k[v_x - j v_y + j\omega_c(x - jy)] \quad , \quad (4.12)
 \end{aligned}$$

A_i = amplitude of the wave, $i = 1, 2, 3, 4$,

$$k = \sqrt{I_0 \omega / 8 \eta \omega_c} \quad , \quad \beta_e = \frac{\omega}{u_0} \quad , \quad \beta_c = \frac{\omega_c}{u_0} \quad ,$$

$$E_{\pm} = E_x \pm j E_y \quad ,$$

$$B_{\pm} = B_x \pm j B_y \quad ,$$

$$\omega_c = \eta B_0 \quad .$$

The transverse displacements and velocities can also be expressed in terms of mode amplitudes by using Eqs. 4.9-4.12, as

$$x = \frac{a_4 - a_2 - a_3 + a_1}{2 j k \omega_c} , \quad (4.13)$$

$$y = \frac{a_4 - a_2 + a_3 - a_1}{2 k \omega_c} , \quad (4.14)$$

$$v_x = \frac{a_1 + a_2}{2 k} \quad (4.15)$$

and

$$v_y = \frac{a_1 - a_2}{2 j k} . \quad (4.16)$$

4.3 Coupled-Mode Analysis of D-c Pumped Quadrupole Amplifiers

4.3.1 General Procedure of the Analysis.

To simplify the analysis of a d-c pumped quadrupole amplifier, let us assume that the a-c magnetic fields in the transverse direction are negligible, i.e., $B_{\pm} = 0$ and that ω_c is a constant and that $dk/dt = 0$. The coupled-mode equations (Eqs. 4.5-4.8) reduce to

$$\left(\frac{d}{dt} - j \omega_c\right) a_1 = - \eta k E_+$$

$$\left(\frac{d}{dt} + j \omega_c\right) a_2 = - \eta k E_-$$

$$\frac{da_3}{dt} = - \eta k E_+$$

$$\frac{da_4}{dt} = - \eta k E_- . \quad (4.17)$$

In order that parametric pumping can be achieved in a d-c pumped quadrupole amplifier, the pump field must be an appropriate function of x, y and z. Let the transverse fields E_+ and E_- be a function of the coordinates of the form,

$$\begin{aligned}
 E_+ &= f_1(x,y) f_2(z) \\
 E_- &= f_3(x,y) f_4(z) .
 \end{aligned}
 \tag{4.18}$$

By means of Eqs. 4.13 and 4.14, it is possible to express E_+ and E_- as a function of the coupled modes a_1 ---, a_4 . Thus, one may write

$$\begin{aligned}
 E_+ &= f_{1+}(a_1, a_2, a_3, a_4) f_2(z) \\
 E_- &= f_{1-}(a_1, a_2, a_3, a_4) f_4(z) .
 \end{aligned}
 \tag{4.19}$$

Hence Eq. 4.17 can be rewritten as

$$\left(\frac{d}{dt} - j\omega_c \right) a_1 = -\eta k f_{1+}(a_1, a_2, a_3, a_4) f_2(z) ,$$

$$\left(\frac{d}{dt} + j\omega_c \right) a_2 = -\eta k f_{1-}(a_1, a_2, a_3, a_4) f_4(z) ,$$

$$\frac{da_3}{dt} = -\eta k f_{1+}(a_1, a_2, a_3, a_4) f_2(z) ,$$

$$\frac{da_4}{dt} = -\eta k f_{1-}(a_1, a_2, a_3, a_4) f_4(z) .
 \tag{4.20}$$

Equations 4.20 enable one to discover which pair of modes has strong coupling. Depending upon the actual field configuration, the f_{1+} and f_{1-} may or may not contain all the terms in a's. By inspecting each part of Eq. 4.20 separately, one may identify which of the pairs of modes are coupled together. This point will be made clearer in an example in a later section.

Equation 4.17 can further be simplified for the case of constant axial velocity and a d-c pumping, i.e., $v_z = u_0 = \text{constant}$ and $\omega = 0$.

Assume sinusoidal variations, then

$$\frac{d}{dt} = j\omega + u_0 \frac{\partial}{\partial z} = u_0 \frac{\partial}{\partial z} .$$

Equation 4.20 becomes

$$\left(\frac{\partial}{\partial z} - j\beta_c \right) a_1 = - \frac{\eta k}{u_0} E_+ , \quad (4.21a)$$

$$\left(\frac{\partial}{\partial z} + j\beta_c \right) a_2 = - \frac{\eta k}{u_0} E_- , \quad (4.21b)$$

$$\frac{\partial a_3}{\partial z} = - \frac{\eta k}{u_0} E_+ , \quad (4.21c)$$

$$\frac{\partial a_4}{\partial z} = - \frac{\eta k}{u_0} E_- . \quad (4.21d)$$

In order to examine the effectiveness of the mode coupling, a set of second-order coupled-mode equations will be derived. Differentiating Eqs. 4.21a and 4.21d, subtract, and then adding Eq. 4.21c which is multiplied by $j\beta_c$, one obtains after some simplifications, the following expression:

$$e^{j\beta_c z} \left(\frac{\partial^2 A_1}{\partial z^2} + j\beta_c \frac{\partial A_1}{\partial z} \right) - \frac{\partial^2 A_3}{\partial z^2} + j\beta_c \frac{\partial A_3}{\partial z} = - j\beta_c \frac{\eta k}{u_0} E_+ . \quad (4.22)$$

Similarly from Eqs. 4.21b and 4.21c, the following is obtained:

$$e^{-j\beta_c z} \left(\frac{\partial^2 A_2}{\partial z^2} - j\beta_c \frac{\partial A_2}{\partial z} \right) - \frac{\partial^2 A_4}{\partial z^2} - j\beta_c \frac{\partial A_4}{\partial z} = j\beta_c \frac{\eta k}{u_0} E_- . \quad (4.23)$$

Equations 4.22 and 4.23 are the general expressions which can be used to analyze all types of d-c pumped amplifiers as long as the pump field E_{\pm} can be determined.

4.3.2 Staggered Quadrupole Amplifier. As a typical example, a detailed discussion based upon Eqs. 4.20, 4.22 and 4.23 will be given for a staggered quadrupole amplifier. The pump electrode configuration of such a device is shown in Fig. 4.1.

The potential in the pump region is given by

$$V(r, \Phi, z) = V_p \left(\frac{r}{a} \right)^2 \cos 2\Phi \cos \beta_q z . \quad (4.24)$$

In rectangular coordinates, the field intensities are

$$\begin{aligned} E_x &= -2 \frac{V_p}{a^2} x \cos \beta_q z , \\ E_y &= 2 \frac{V_p}{a^2} y \cos \beta_q z , \end{aligned} \quad (4.25)$$

where $\beta_q = 2\pi/L$.

Then

$$\begin{aligned} E_+ &= j \frac{2V_p}{a^2 k \omega_c} (a_4 - a_2) \cos \beta_q z , \\ E_- &= -j \frac{2V_p}{a^2 k \omega_c} (a_1 - a_3) \cos \beta_q z . \end{aligned} \quad (4.26)$$

Substituting these quantities into Eqs. 4.20, one obtains

$$\left(\frac{d}{dt} - j \omega_c \right) a_1 = -j \frac{2\eta V_p}{a^2 \omega_c} (a_4 - a_2) \cos \beta_q z , \quad (4.27a)$$

$$\left(\frac{d}{dt} + j \omega_c \right) a_2 = -j \frac{2\eta V_p}{a^2 \omega_c} (a_1 - a_3) \cos \beta_q z , \quad (4.27b)$$

$$\frac{da_3}{dt} = -j \frac{2\eta V_p}{a^2 \omega_c} (a_4 - a_2) \cos \beta_q z , \quad (4.27c)$$

$$\frac{da_4}{dt} = -j \frac{2\eta V_p}{a^2 \omega_c} (a_1 - a_3) \cos \beta_q z . \quad (4.27d)$$

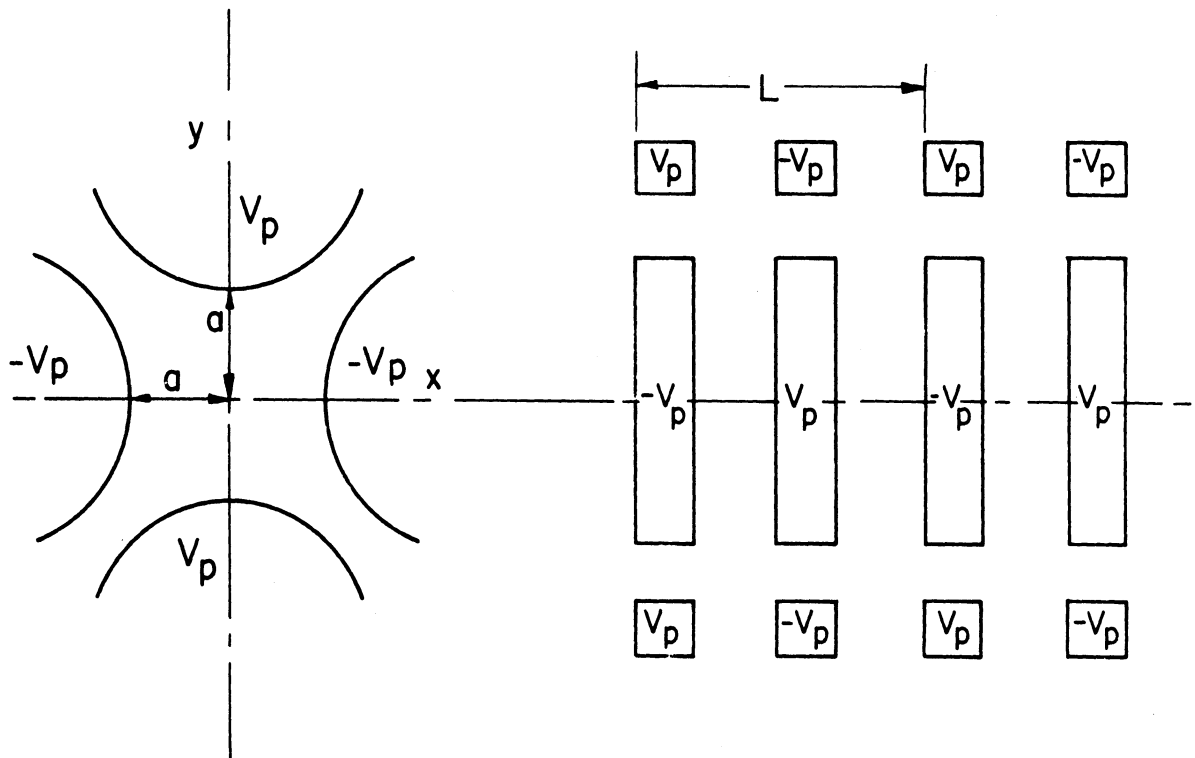


FIG. 4.1 GEOMETRICAL CONFIGURATIONS OF A STAGGERED QUADRUPOLE PUMP STRUCTURE.

The important feature of the parametric coupling can readily be seen from this set of equations. With a staggered quadrupole d-c pump field, the following mode couplings are possible, Eq. 4.27a indicates the possible coupling between the fast cyclotron wave a_1 to the slow cyclotron wave a_2 and the positive synchronous wave a_4 , similar coupling pairs can be sorted out easily from the other equations. However, two types of coupling are not possible, namely, a_1 and a_3 , and a_2 and a_4 .

Let us proceed to study the different cases of couplings more carefully. Substituting the fields E_+ and E_- for the staggered quadrupole of Eq. 4.26 into Eqs. 4.22 and 4.23, one obtains

$$\left(\frac{\partial^2 A_1}{\partial z^2} + j\beta_c \frac{\partial A_1}{\partial z} \right) e^{j\beta_c z} - \frac{\partial^2 A_3}{\partial z^2} + j\beta_c \frac{\partial A_3}{\partial z} = M \left[A_4 e^{j\beta_q z} + A_4 e^{-j\beta_q z} - A_2 e^{j(\beta_q - \beta_c)z} - A_2 e^{-j(\beta_q + \beta_c)z} \right] \quad (4.28)$$

and

$$\left(\frac{\partial^2 A_2}{\partial z^2} - j\beta_c \frac{\partial A_2}{\partial z} \right) e^{-j\beta_c z} - \frac{\partial^2 A_4}{\partial z^2} - j\beta_c \frac{\partial A_4}{\partial z} = M \left[A_3 e^{j\beta_q z} + A_3 e^{-j\beta_q z} - A_1 e^{j(\beta_q + \beta_c)z} - A_1 e^{-j(\beta_q - \beta_c)z} \right], \quad (4.29)$$

where $M = (V_p \eta \beta_c / u_0 \omega_c a^2) = (V_p / 2V_0 a^2)$, and the A's are the amplitudes of the coupled modes.

Equations 4.28 and 4.29 may be used to discuss the coupling modes and the gain of the device. There are several cases of interest

depending upon the spacing between the quadrupole sections, which can be discussed separately.

Case I. Coupling between Cyclotron Waves.

Let the spacing $L = \lambda_c/2$ or $\beta_q = 2\beta_c$

Equations 4.28 and 4.29 become

$$\left[\frac{\partial^2 A}{\partial z^2} + j\beta_c \frac{\partial A}{\partial z} \right] e^{j\beta_c z} - \frac{\partial^2 A}{\partial z^2} + j\beta_c \frac{\partial A}{\partial z} = MA_4 e^{j2\beta_c z} + MA_4 e^{-j2\beta_c z} - MA_2 e^{j\beta_c z} - MA_2 e^{-j\beta_c z}, \quad (4.30)$$

$$\left[\frac{\partial^2 A}{\partial z^2} - j\beta_c \frac{\partial A}{\partial z} \right] e^{-j\beta_c z} - \frac{\partial^2 A}{\partial z^2} - j\beta_c \frac{\partial A}{\partial z} = MA_3 e^{j2\beta_c z} + MA_3 e^{-2j\beta_c z} - MA_1 e^{j\beta_c z} - MA_1 e^{-j\beta_c z}. \quad (4.31)$$

Equating z-dependence terms,

$$\frac{\partial^2 A}{\partial z^2} + j\beta_c \frac{\partial A}{\partial z} = -MA_2, \quad (4.32a)$$

$$\frac{\partial^2 A}{\partial z^2} - j\beta_c \frac{\partial A}{\partial z} = -MA_1, \quad (4.32b)$$

$$\frac{\partial^2 A}{\partial z^2} - j\beta_c \frac{\partial A}{\partial z} = 0, \quad (4.32c)$$

$$\frac{\partial^2 A}{\partial z^2} + j\beta_c \frac{\partial A}{\partial z} = 0. \quad (4.32d)$$

It is obvious that there is no coupling for the synchronous waves, but the fast and slow cyclotron waves are closely coupled.

The roots of Eqs. 4.32a and 4.32b are

$$\gamma_1 = \frac{\beta_c}{\sqrt{2}} \sqrt{-1 + \sqrt{1 + 4 (M/\beta_c^2)^2}} , \quad (4.33a)$$

$$\gamma_2 = j \frac{\beta_c}{\sqrt{2}} \sqrt{1 + \sqrt{1 + 4 (M/\beta_c^2)^2}} = j\beta_2 , \quad (4.33b)$$

$$\gamma_3 = \frac{\beta_c}{\sqrt{2}} \sqrt{-1 + \sqrt{1 + 4 (M/\beta_c^2)^2}} = -\gamma_1 , \quad (4.33c)$$

$$\gamma_4 = -j \frac{\beta_c}{\sqrt{2}} \sqrt{1 + \sqrt{1 + 4 (M/\beta_c^2)^2}} = -j\beta_2 , \quad (4.33d)$$

where

$$\beta_2 \triangleq \frac{\beta_c}{\sqrt{2}} \sqrt{1 + \sqrt{1 + 4 (M/\beta_c^2)^2}} .$$

It is noticed that γ_1 is a positive real quantity for all possible M's (M varies as V_p varies) and γ_2 is pure imaginary. $\gamma_3 = -\gamma_1$ and $\gamma_4 = -\gamma_2$. It is clear that a growing wave is possible in this case.

The solutions for the fast cyclotron wave a_1 and its slow cyclotron wave a_2 are, respectively,

$$\begin{aligned} a_1 &= A_1 e^{j\beta_c z} \\ &= (f_{11} e^{\gamma_1 z} + f_{12} e^{j\beta_2 z} + f_{13} e^{-\gamma_1 z} + f_{14} e^{-j\beta_2 z}) e^{j\beta_c z} \end{aligned} \quad (4.34)$$

and

$$\begin{aligned}
 a_2 &= A_2 e^{j\beta_c z} \\
 &= (f_{21} e^{\gamma z} + f_{22} e^{j\beta_c z} + f_{23} e^{-\gamma z} + f_{24} e^{-j\beta_c z}) e^{-j\beta_c z} . \quad (4.35)
 \end{aligned}$$

It is noticed that there are four component waves in each mode; one is a growing wave, one is a decaying wave and the other two waves are constant amplitude waves with phase velocities corresponding to $\beta_2 \pm \beta_c$ respectively. The phase constants of these component waves are plotted in Fig. 4.2 as a function of the pumping parameter M. The amplitude gain of the growing wave vs. pumping parameter M is shown in Fig. 4.3.

Case II. Coupling between Synchronous Waves.

Let the spacing $L \rightarrow \infty$ (i.e., single extended section).

$$\beta_q = \frac{2\pi}{L} = 0 .$$

From Eqs. 4.28 and 4.29, one obtains

$$\begin{aligned}
 \left[\frac{\partial^2 A_1}{\partial z^2} + j\beta_c \frac{\partial A_1}{\partial z} \right] e^{j\beta_c z} - \frac{\partial^2 A_3}{\partial z^2} + j\beta_c \frac{\partial A_3}{\partial z} \\
 = 2M (A_4 - A_2 e^{-j\beta_c z}) \quad (4.36)
 \end{aligned}$$

and

$$\left[\frac{\partial^2 A_2}{\partial z^2} - j\beta_c \frac{\partial A_2}{\partial z} \right] e^{-j\beta_c z} - \frac{\partial^2 A_4}{\partial z^2} - j\beta_c \frac{\partial A_4}{\partial z} = 2M (A_3 - A_1 e^{j\beta_c z}) . \quad (4.37)$$

Thus,

$$\frac{\partial^2 A_1}{\partial z^2} + j\beta_c \frac{\partial A_1}{\partial z} = 0 , \quad (4.38a)$$

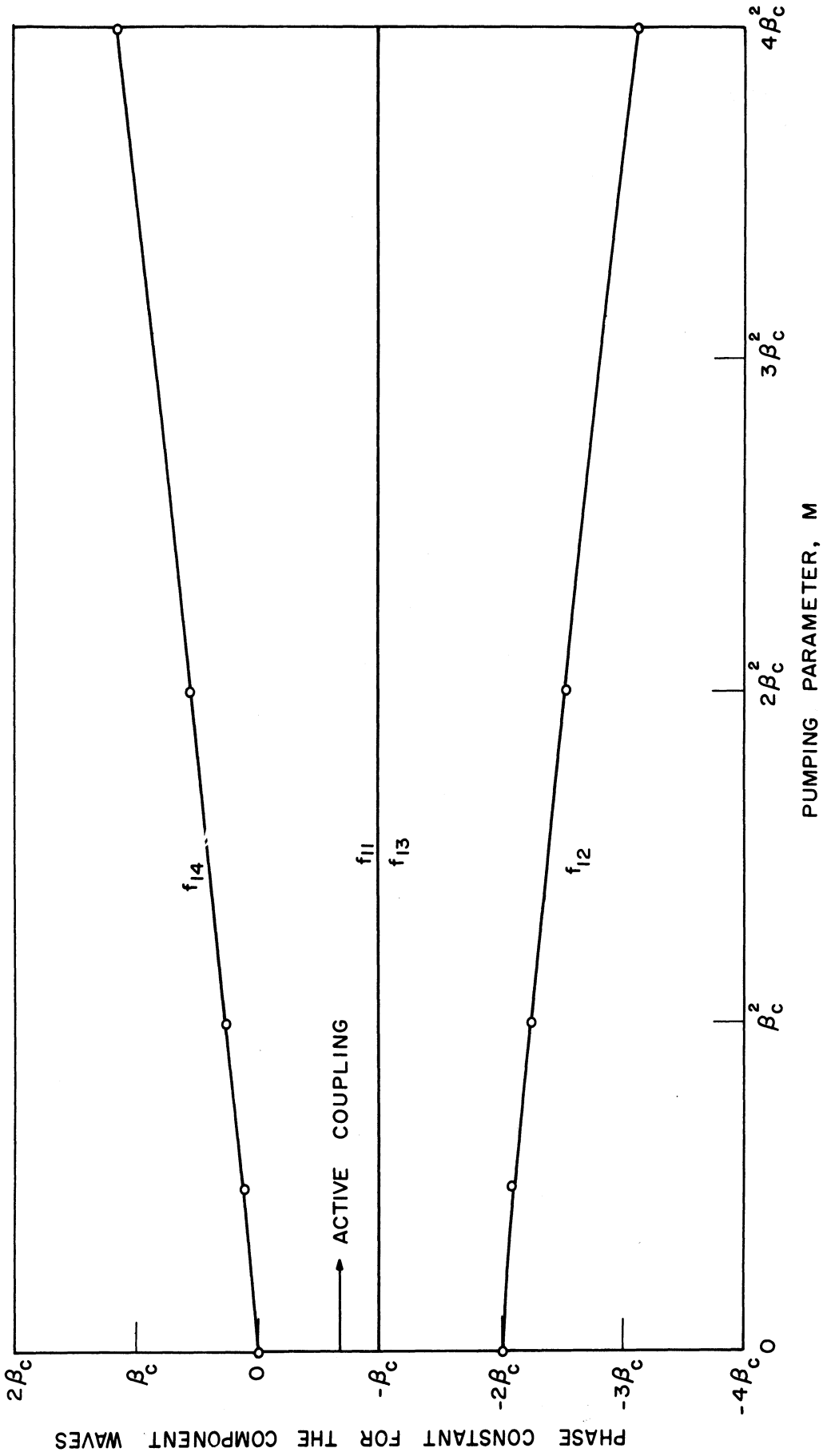


FIG. 4.2 PHASE CONSTANT VS. PUMPING PARAMETER M FOR THE FAST CYCLOTRON WAVE IN A STAGGERED QUADRUPOLE PUMP STRUCTURE. $\beta_q = 2\beta_c$, FAST AND SLOW CYCLOTRON WAVE INTERACTION.

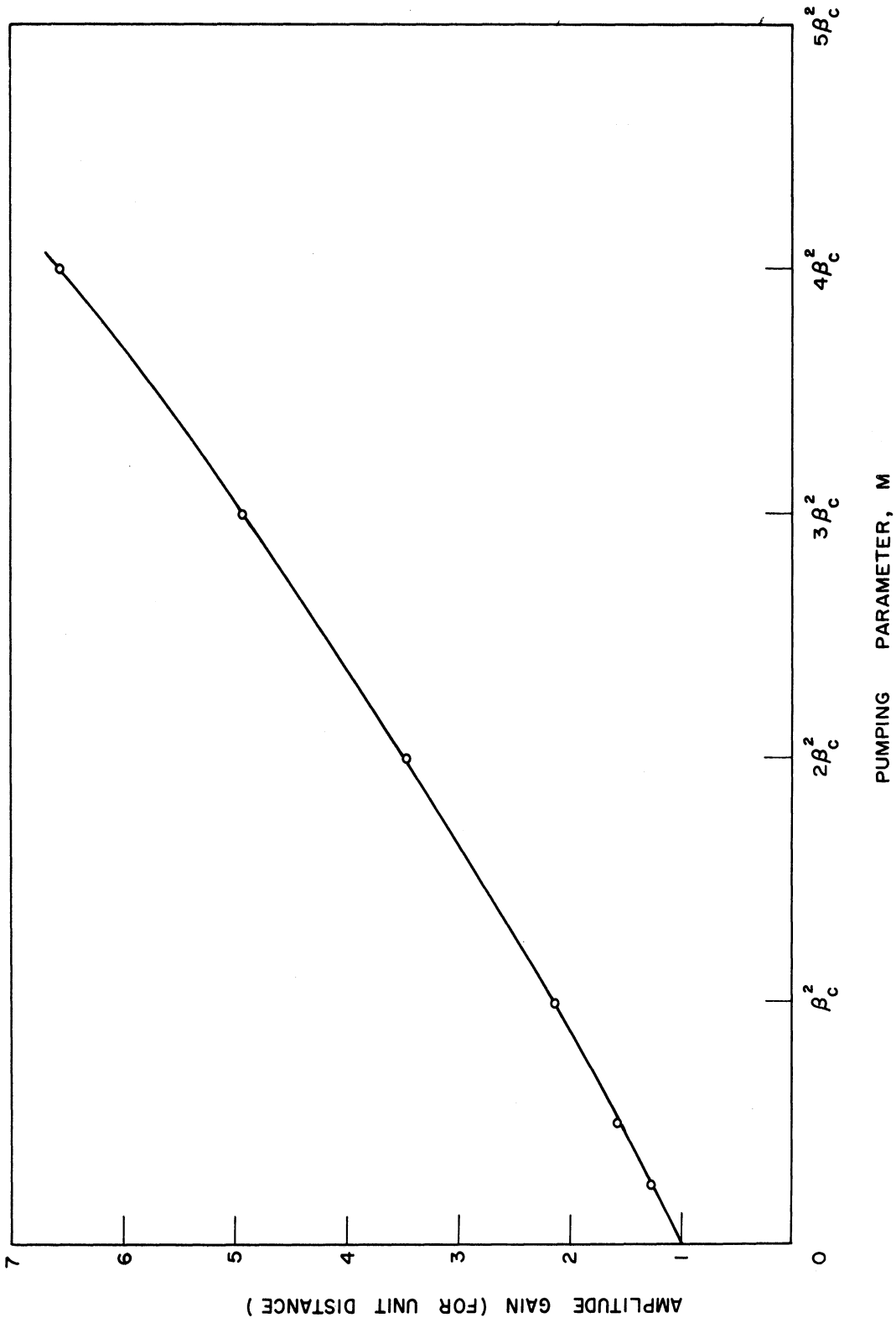


FIG. 4.3 AMPLITUDE GAIN VS. PUMPING PARAMETER M FOR THE FAST CYCLOTRON WAVE IN A STAGGERED QUADRUPOLE PUMP STRUCTURE. $\beta_q = 2\beta_c$, FAST AND SLOW CYCLOTRON WAVE INTERACTION.

$$\frac{\partial^2 A}{\partial z^2} - j\beta_c \frac{\partial A}{\partial z} = 0 \quad , \quad (4.38b)$$

$$\frac{\partial^2 A}{\partial z^2} - j\beta_c \frac{\partial A}{\partial z} = -2MA_4 \quad , \quad (4.38c)$$

$$\frac{\partial^2 A}{\partial z^2} + j\beta_c \frac{\partial A}{\partial z} = -2MA_3 \quad . \quad (4.38d)$$

It can be seen that there is no coupling for the fast and slow cyclotron waves, while there is coupling between the synchronous waves.

The propagation constants are found to be

$$\gamma_1 = \frac{\beta_c}{\sqrt{2}} \sqrt{-1 + \sqrt{1 + (4M/\beta_c^2)^2}} \quad , \quad (4.39a)$$

$$\gamma_2 = -\frac{\beta_c}{\sqrt{2}} \sqrt{-1 + \sqrt{1 + (4M/\beta_c^2)^2}} = -\gamma_1 \quad , \quad (4.39b)$$

$$\gamma_3 = j \frac{\beta_c}{\sqrt{2}} \sqrt{1 + \sqrt{1 + (4M/\beta_c^2)^2}} = j\beta_2 \quad , \quad (4.39c)$$

$$\gamma_4 = -j \frac{\beta_c}{\sqrt{2}} \sqrt{1 + \sqrt{1 + (4M/\beta_c^2)^2}} = -j\beta_2 \quad . \quad (4.39d)$$

They are of the similar form as in the previous case and thus gain can be obtained in this case.

Case III. Coupling between Cyclotron and Synchronous Waves.

Let the spacing L be equal to the cyclotron wavelength λ_c ; then, $\beta_q = \beta_c$. Equations 4.28 and 4.29 become

$$\left[\frac{\partial^2 A_1}{\partial z^2} + j\beta_c \frac{\partial A_1}{\partial z} \right] e^{+j\beta_c z} - \frac{\partial^2 A_3}{\partial z^2} + j\beta_c \frac{\partial A_3}{\partial z}$$

$$= M \left[A_4 e^{j\beta_c z} + A_4 e^{-j\beta_c z} - A_2 - A_2 e^{-j2\beta_c z} \right] \quad (4.40)$$

and

$$\left[\frac{\partial^2 A_2}{\partial z^2} - j\beta_c \frac{\partial A_2}{\partial z} \right] e^{-j\beta_c z} - \frac{\partial^2 A_4}{\partial z^2} - j\beta_c \frac{\partial A_4}{\partial z}$$

$$= M \left[A_3 e^{j\beta_c z} + A_3 e^{-j\beta_c z} - A_1 e^{j2\beta_c z} - A_1 \right] . \quad (4.41)$$

Equating the corresponding z-dependence terms, one obtains

$$\frac{\partial^2 A_1}{\partial z^2} + j\beta_c \frac{\partial A_1}{\partial z} = M A_4 , \quad (4.42a)$$

$$\frac{\partial^2 A_4}{\partial z^2} + j\beta_c \frac{\partial A_4}{\partial z} = M A_1 , \quad (4.42b)$$

$$\frac{\partial^2 A_2}{\partial z^2} - j\beta_c \frac{\partial A_2}{\partial z} = M A_3 , \quad (4.42c)$$

$$\frac{\partial^2 A_3}{\partial z^2} - j\beta_c \frac{\partial A_3}{\partial z} = M A_2 . \quad (4.42d)$$

1. Coupling between fast cyclotron wave and positive kinetic power synchronous wave.

The coupling between A_1 and A_4 can be analyzed in the following manner. By solving simultaneously Eqs. 4.42a and 4.42b, one finds the roots of γ of the characteristic equation $(\gamma^2 + j\beta_c \gamma)^2 - M^2 = 0$ as

$$\gamma_1 = -j \frac{\beta_c}{2} (1 - \sqrt{1 - (4M/\beta_c^2)}) , \quad (4.43a)$$

$$\gamma_2 = -j \frac{\beta_c}{2} (1 + \sqrt{1 - (4M/\beta_c^2)}) , \quad (4.43b)$$

$$\gamma_3 = -j \frac{\beta_c}{2} (1 - \sqrt{1 + (4M/\beta_c^2)}) , \quad (4.43c)$$

$$\gamma_4 = -j \frac{\beta_c}{2} (1 + \sqrt{1 + (4M/\beta_c^2)}) , \quad (4.43d)$$

There are two possible cases of operation:

a. For $M < \beta_c^2/4$, all four γ 's are pure imaginary, the amplitudes of the component waves are constant. A_1 and A_4 are said to be coupled passively.

b. For $M > \beta_c^2/4$, γ_1 has a positive real part, which indicates that f_{11} and f_{41} are growing waves, therefore, gain can be obtained.

The ω - β diagram for both cases are shown in Figs. 4.4 and 4.5.

The phase constant for the component waves as a function of pumping parameter M is shown in Fig. 4.6. Notice that for $M > \beta_c^2/4$ the component waves f_{11} , f_{12} , have constant $\beta = -\beta_c/2$, and have growing and decaying amplitudes.

2. Coupling between slow cyclotron wave and negative (kinetic power) synchronous wave. Consider Eqs. 4.42c and 4.42d, the propagation constants are found to be

$$\gamma_1 = j \frac{\beta_c}{2} (1 - \sqrt{1 - (4M/\beta_c^2)}) \quad (4.44a)$$

$$\gamma_2 = j \frac{\beta_c}{2} (1 + \sqrt{1 - (4M/\beta_c^2)}) , \quad (4.44b)$$

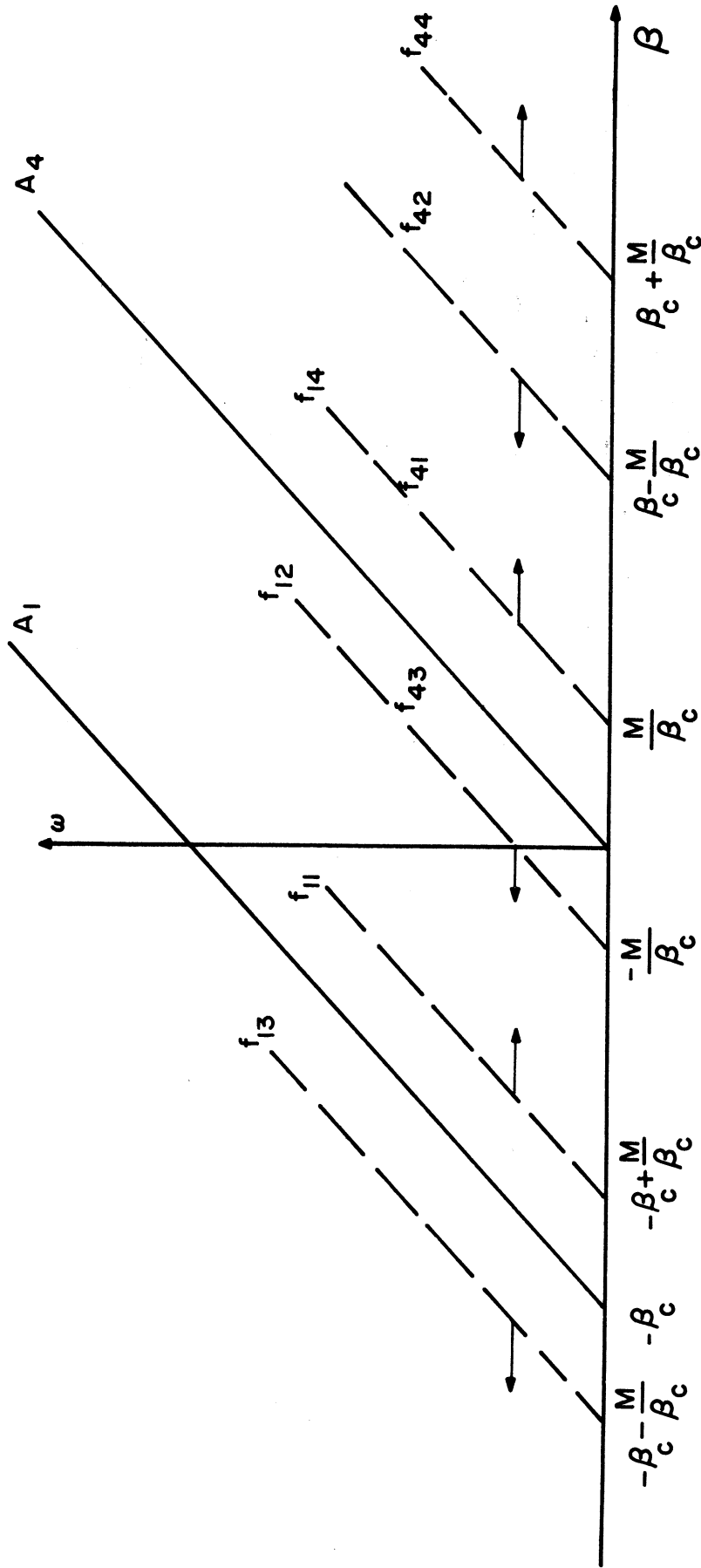


FIG. 4.4 ω - β PLOT OF THE CYCLOTRON-TO-SYNCHRONOUS WAVE INTERACTION IN A STAGGERED QUADRUPOLE PUMP STRUCTURE, PASSIVE COUPLING.

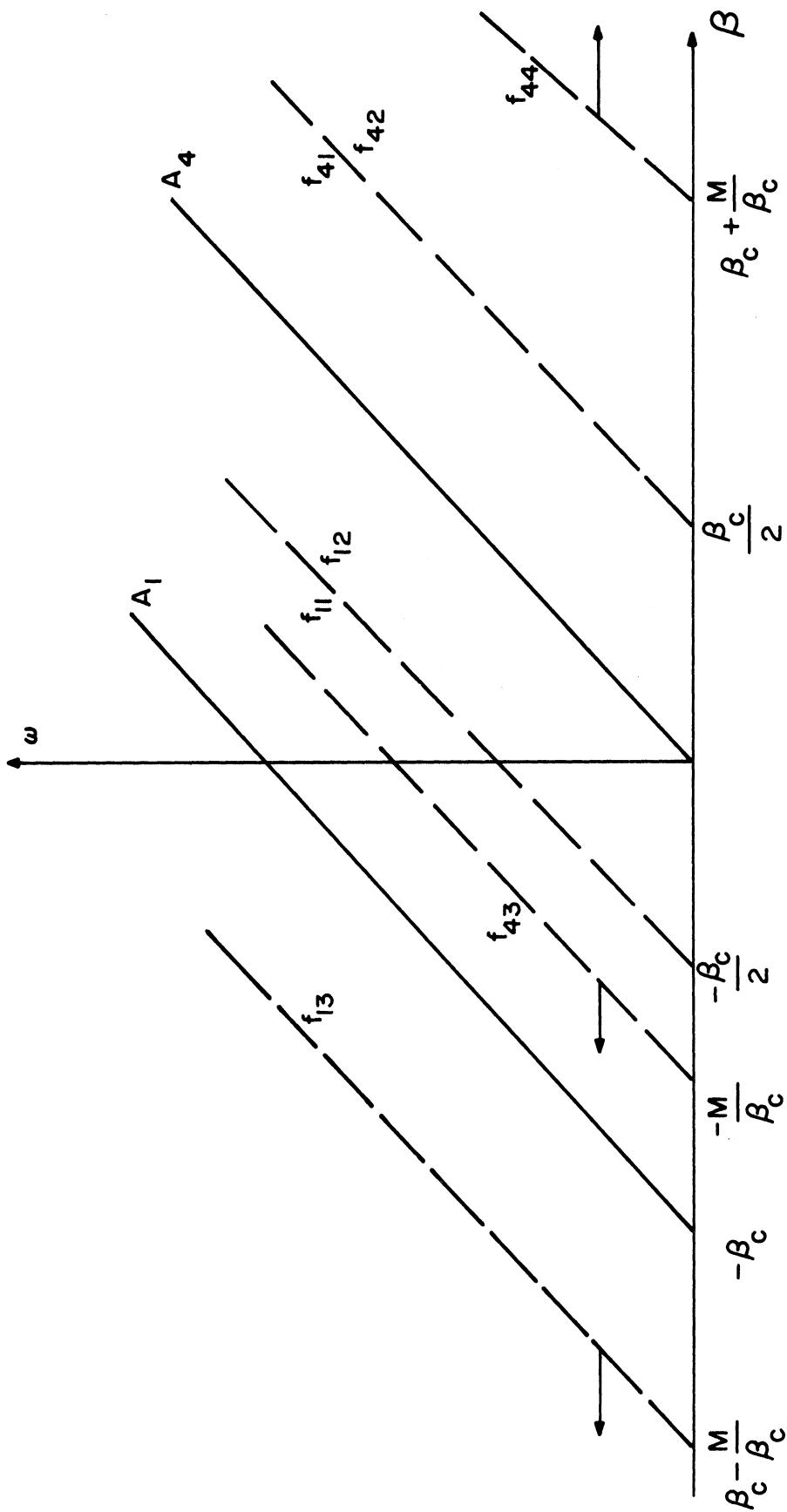


FIG. 4.5 ω - β PLOT OF THE CYCLOTRON-TO-SYNCHRONOUS WAVE INTERACTION IN A STAGGERED QUADRUPOLE PUMP STRUCTURE, ACTIVE COUPLING.

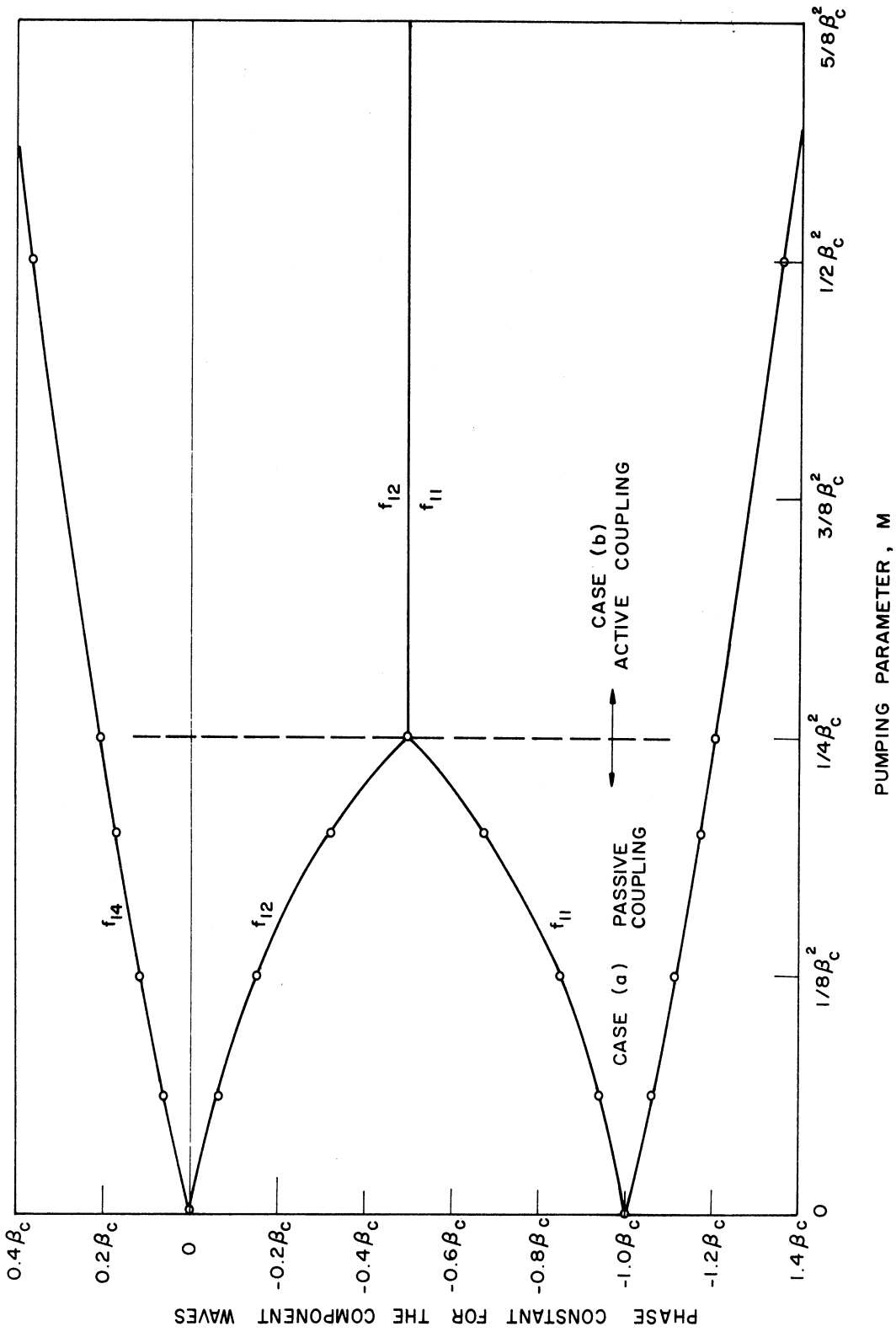


FIG. 4.6 PHASE CONSTANT VS. PUMPING PARAMETER M FOR THE FAST CYCLOTRON WAVE IN A STAGGERED QUADRUPOLE PUMP STRUCTURE. $\beta_q = \beta_c$ FAST CYCLOTRON-TO-SYNCHRONOUS WAVE INTERACTION.

$$\gamma_3 = j \frac{\beta_c}{2} (1 - \sqrt{1 + (4M/\beta_c^2)}) , \quad (4.44c)$$

$$\gamma_4 = j \frac{\beta_c}{2} (1 + \sqrt{1 + (4M/\beta_c^2)}) . \quad (4.44d)$$

Again there are two possibilities as in (1), when $4M/\beta_c^2 > 1$ gain is observed.

4.3.3 Other Pumping Fields.

4.3.3a Twisted Quadrupole Pump Structure. Figure 4.7a shows the geometrical configuration of a twisted quadrupole pump structure.

The equation of the potential in rectangular coordinate system is

$$V = -\frac{1}{2} \frac{V_p}{a^2} [(x^2 - y^2) \sin 2\beta z - 2xy \cos 2\beta z] . \quad (4.45)$$

The equations of the polarized field in terms of the coupled modes are

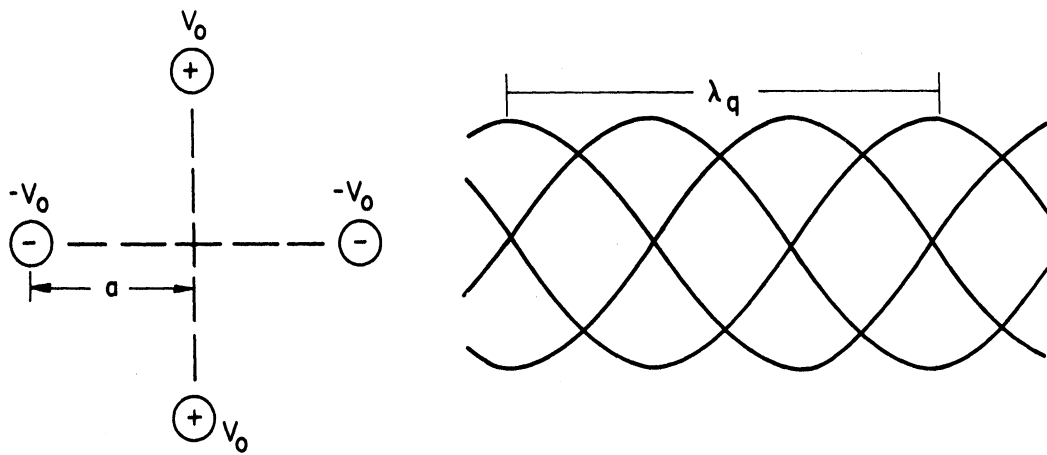
$$E_+ = -\frac{V_p}{k\omega_c a^2} (a_4 - a_2) e^{j2\beta_q z} ,$$

$$E_- = -\frac{V_p}{k\omega_c a^2} (a_3 - a_1) e^{-j2\beta_q z} . \quad (4.46)$$

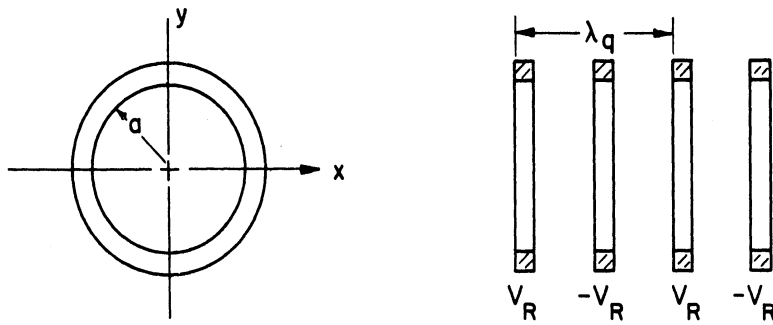
The propagation constants for coupling between the fast and slow cyclotron waves for

$$\beta_q = \beta_c \text{ coupling between } A_1 \text{ and } A_2$$

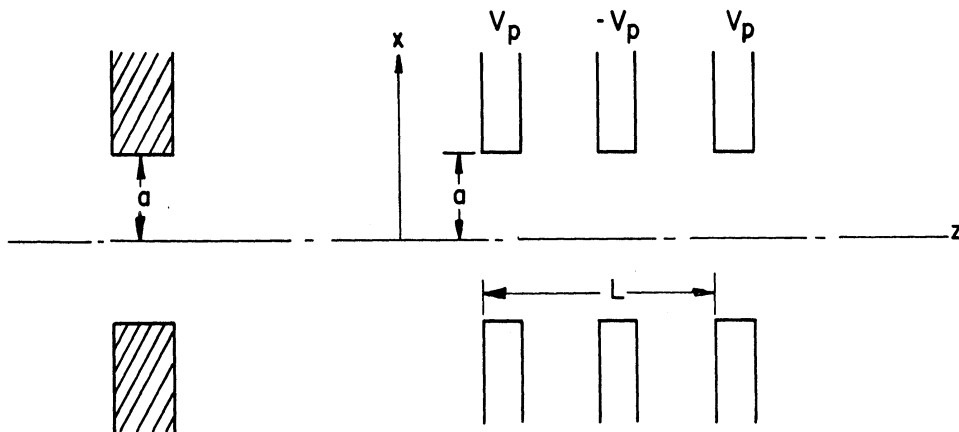
are



a) TWISTED QUADRUPOLE STRUCTURE



b) PERIODIC RING STRUCTURE



c) ELECTROSTATIC SLOT STRUCTURE

FIG. 4.7 GEOMETRICAL CONFIGURATIONS OF (a) TWISTED QUADRUPOLE-TYPE, (b) PERIODIC RING-TYPE AND (c) PERIODIC SLOT-TYPE OF QUADRUPOLE PUMP STRUCTURES.

$$\gamma_{1,3} = \pm \frac{\beta_c}{\sqrt{2}} \sqrt{-1 + \sqrt{1 + 4(M/\beta_c)^2}} = \pm \gamma ,$$

$$\gamma_{2,4} = \pm j \frac{\beta_c}{\sqrt{2}} \sqrt{1 + \sqrt{1 + 4(M/\beta_c)^2}} = \pm j\beta_2 . \quad (4.47)$$

For the coupling between synchronous waves A_3 and A_4 , $\beta_q = 0$, and $\lambda_q = \infty$.

Roots of the propagation constant γ are the same as in the previous case, indicating the possibility of obtaining gain.

For the coupling between cyclotron and synchronous waves,

$$\beta_q = \frac{1}{2} \beta_c , \lambda_q = 2\lambda_c .$$

For the coupling between A_1 and A_4 ,

$$\gamma_{1,2} = -j \frac{\beta_c}{2} (1 \mp \sqrt{1 - (4M/\beta_c^2)}) ,$$

$$\gamma_{3,4} = -j \frac{\beta_c}{2} (1 \mp \sqrt{1 + (4M/\beta_c^2)}) . \quad (4.48)$$

It can be seen from this equation that the passive coupling occurs for $4M/\beta_c^2 < 1$, and the conditional coupling occurs for $4M/\beta_c^2 > 1$.

For the coupling between A_2 and A_3 , the same criterion applies.

4.3.3b Periodic Ring Quadrupole Structure. Figure 4.7b shows the geometrical configuration of a periodic ring-type quadrupole pump structure.

The equation of the potential is

$$V = \frac{1}{2} \frac{V_p}{a^2} (x^2 + y^2) \sin \beta_q z . \quad (4.49)$$

The equations of the transverse polarized field in terms of the coupled modes are

$$\begin{aligned} E_+ &= j \frac{V_p}{k\omega_c a^2} (a_3 - a_1) \sin \beta_q z , \\ E_- &= -j \frac{V_p}{k\omega_c a^2} (a_4 - a_2) \sin \beta_q z . \end{aligned} \quad (4.50)$$

The propagation constants for coupling between cyclotron and synchronous waves are

$$\beta_q = \beta_c ,$$

$$\begin{aligned} \gamma_1 &= \pm \frac{\beta_c}{\sqrt{2}} \sqrt{-1 + \sqrt{1 + 4(N/\beta_c^2)^2}} = \pm \gamma . \\ \gamma_2 & \end{aligned} \quad (4.51a)$$

γ is real for all possible N , and

$$\begin{aligned} \gamma_3 &= \pm \frac{\beta_c}{\sqrt{2}} \sqrt{1 + \sqrt{1 + 4(N/\beta_c^2)^2}} = \pm j\beta_2 , \\ \gamma_4 & \end{aligned} \quad (4.51b)$$

where

$$N = \frac{\eta V_p}{2u_0 \omega_c a^2} \beta_c .$$

A_1 and A_3 can be actively coupled, and A_2 and A_4 can also be actively coupled.

4.3.3c Electrostatic Slot Pump Field Structure. Figure

4.7c shows the geometrical configuration of an electrostatic slot pump field structure.

The equation of the potential in the slot region is

$$V_s = V_o + \sum_{n=1}^{\infty} K_n V_p \frac{\coth \beta_n x}{\coth \beta_n a} \sin \beta_n z, \quad (4.52)$$

where K_n is an amplitude coefficient and V_o is the potential in the absence of the pump field. Consider only the fundamental component of the potential

$$V_s = V_o + V_p \frac{\coth \beta_q x}{\coth \beta_q a} \sin \beta_q z. \quad (4.53)$$

The equation of the transverse polarized field is

$$\begin{aligned} E+ \\ E- \end{aligned} = j \frac{V_p}{2} \frac{\beta_q^2 x}{\coth \beta_q a} (e^{j\beta_q z} - e^{-j\beta_q z}). \quad (4.54)$$

The propagation constants for coupling between A_1 and A_3 , A_1 and A_2 are

$$\begin{aligned} \gamma_1 \\ \gamma_3 \end{aligned} = \pm \frac{\beta_c}{2} \sqrt{-1 + \sqrt{1 + 4 (w/\beta_c^2)^2}}, \quad (4.55a)$$

$$\begin{aligned} \gamma_2 \\ \gamma_4 \end{aligned} = \pm j \frac{\beta_c}{2} \sqrt{1 + \sqrt{1 + 4 (w/\beta_c^2)^2}}, \quad (4.55b)$$

where

$$W = \frac{\beta_c \eta V_p \beta_q^2}{4\omega_c u_o \cosh \beta_q a}.$$

In this case gain is possible.

4.3.4 Gain Computation of the D-c Pumped Amplifiers. To compute the gain, one needs only to consider the exponential amplifying and decaying component of the wave. One may write

$$\begin{aligned} A_1(z) &= B_{11} e^{\gamma z} + \beta_{12} e^{-\gamma z}, \\ A_2(z) &= \beta_{21} e^{\gamma z} + \beta_{22} e^{-\gamma z}, \end{aligned} \quad (4.56)$$

where B_{ij} are the amplitudes to be evaluated from the boundary conditions and

$$\begin{aligned} \gamma_1 &= \frac{\beta_c}{2} \sqrt{-1 + \sqrt{1 + 4(M/\beta_c^2)^2}} \\ &\approx \frac{M}{\beta_c} \text{ for } 4(M/\beta_c^2)^2 \ll 1. \end{aligned}$$

Now

$$A_1(0) = \beta_{11} + \beta_{12}, \quad A_2(0) = \beta_{21} + \beta_{22}$$

and from the original differential equations,

$$\beta_{21} = -j\beta_{11}, \quad \beta_{22} = j\beta_{12}.$$

Solve β_{ij} in terms of $A_1(0)$ and $A_2(0)$ and substituting into Eq. 4.56

$$\begin{aligned} A_1(z) &= A_1(0) \cosh \frac{M}{\beta_c} z + jA_2(0) \sinh \frac{M}{\beta_c} z, \\ A_2(z) &= -A_1(0) \sinh \frac{M}{\beta_c} z + A_2(0) \cosh \frac{M}{\beta_c} z. \end{aligned} \quad (4.57)$$

The gain for the fast cyclotron wave is

$$G_f = \frac{A_1(z)}{A_1(0)} = \cosh \frac{M}{\beta_c} z = \cosh \frac{\eta V_p}{u_o \omega_c a^2} z. \quad (4.58)$$

For $2n$ sections, at the output

$$z = \frac{2n\pi}{\beta_q} = \frac{2n\pi}{2\beta_c} = \frac{n\pi}{\beta_c},$$

$$G_f = \cosh \frac{\eta V_p n\pi}{\omega_c^2 a^2}, \quad (4.59)$$

or the gain in db is

$$G_{fdb} = 20 \log \cosh \frac{\eta V_p n\pi}{\omega_c^2 a^2}. \quad (4.60)$$

The gain for other types of quadrupole structures and coupled modes are computed and tabulated in Table 4.1. For the purpose of comparison, two sets of plots are presented in Figs. 4.8 - 4.10. In Fig. 4.8, the fast cyclotron to slow cyclotron wave coupled modes for different pump structures are compared. Here, the gains in db are plotted against the pump voltage for a constant set of parameters V_0 , β_c , a and n . It is obvious that the twisted quadrupole structure offers the highest gain for the same pump voltage. In Fig. 4.9, the synchronous-to-synchronous wave coupled modes are compared in a similar way. Here the staggered quadrupole shows advantages compared to the twisted quadrupole. In Fig. 4.10 cyclotron-to-synchronous coupled modes are compared. Here, an interesting case can be pointed out. For example, in the case of using staggered quadrupole structure, (see Eq. 4.43), the coupling becomes active only when condition $4M/\beta_c^2 > 1$ is satisfied. Under this condition, the gain is found to be

$$G(\text{db}) = 20 \log_{10} \cosh n\pi \sqrt{(2V_p/v_0 a^2 \beta_c^2) - 1}. \quad (4.61)$$

The comparisons with other structures for similar sets of constants are obvious.

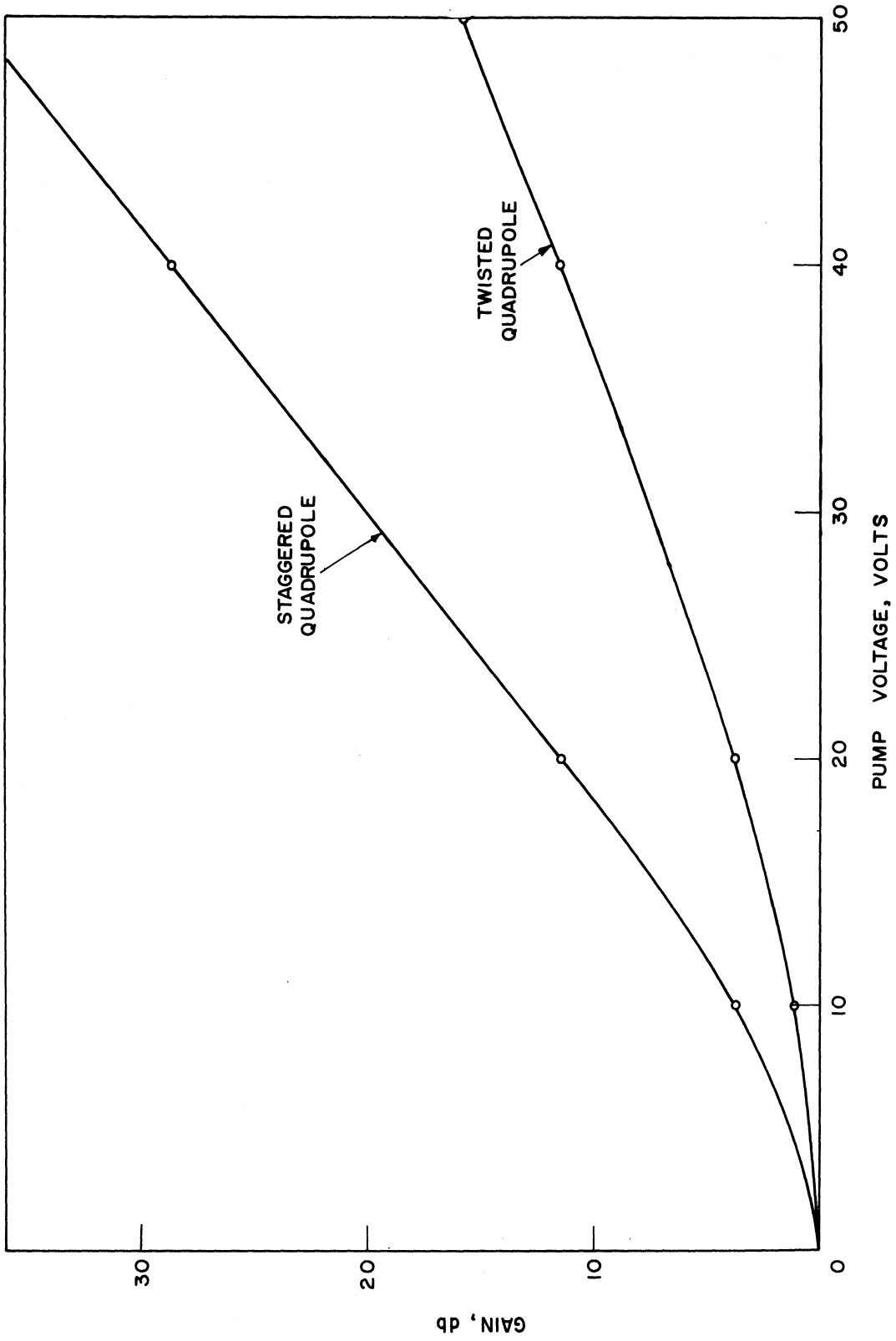


FIG. 4.8 GAIN VS. PUMP VOLTAGE FOR CYCLOTRON-TO-CYCLOTRON TYPE OF INTERACTION IN DIFFERENT

PUMP FIELDS FOR $V_0 = 100$ VOLTS, $\beta_c a = 1$, AND $n = 4$.

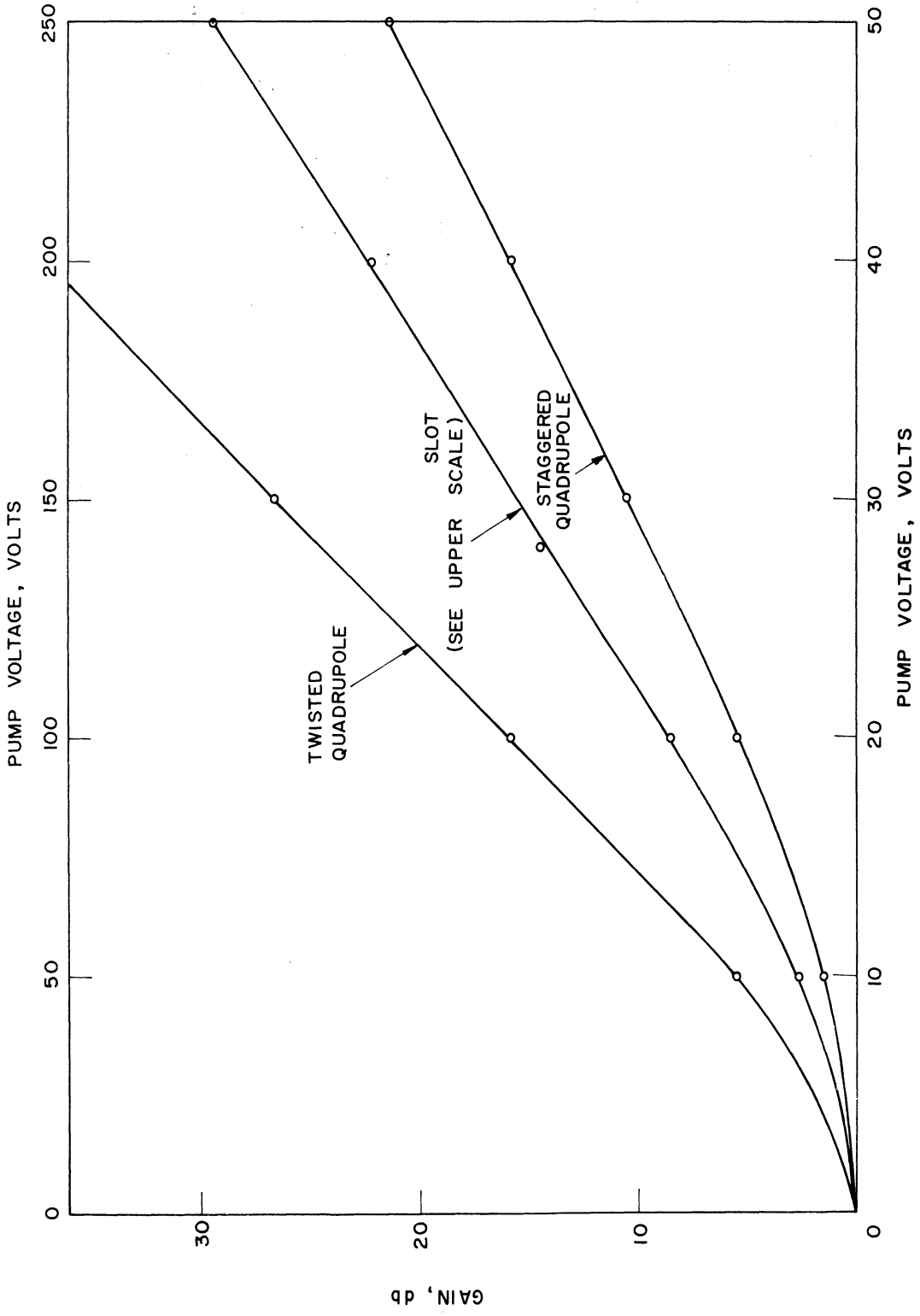


FIG. 4.9 GAIN VS. PUMP VOLTAGE FOR SYNCHRONOUS-TO-SYNCHRONOUS TYPE OF INTERACTION IN DIFFERENT

PUMP FIELDS FOR $V_0 = 100$ VOLTS, $\beta_a = 1$, AND $n = 4$.

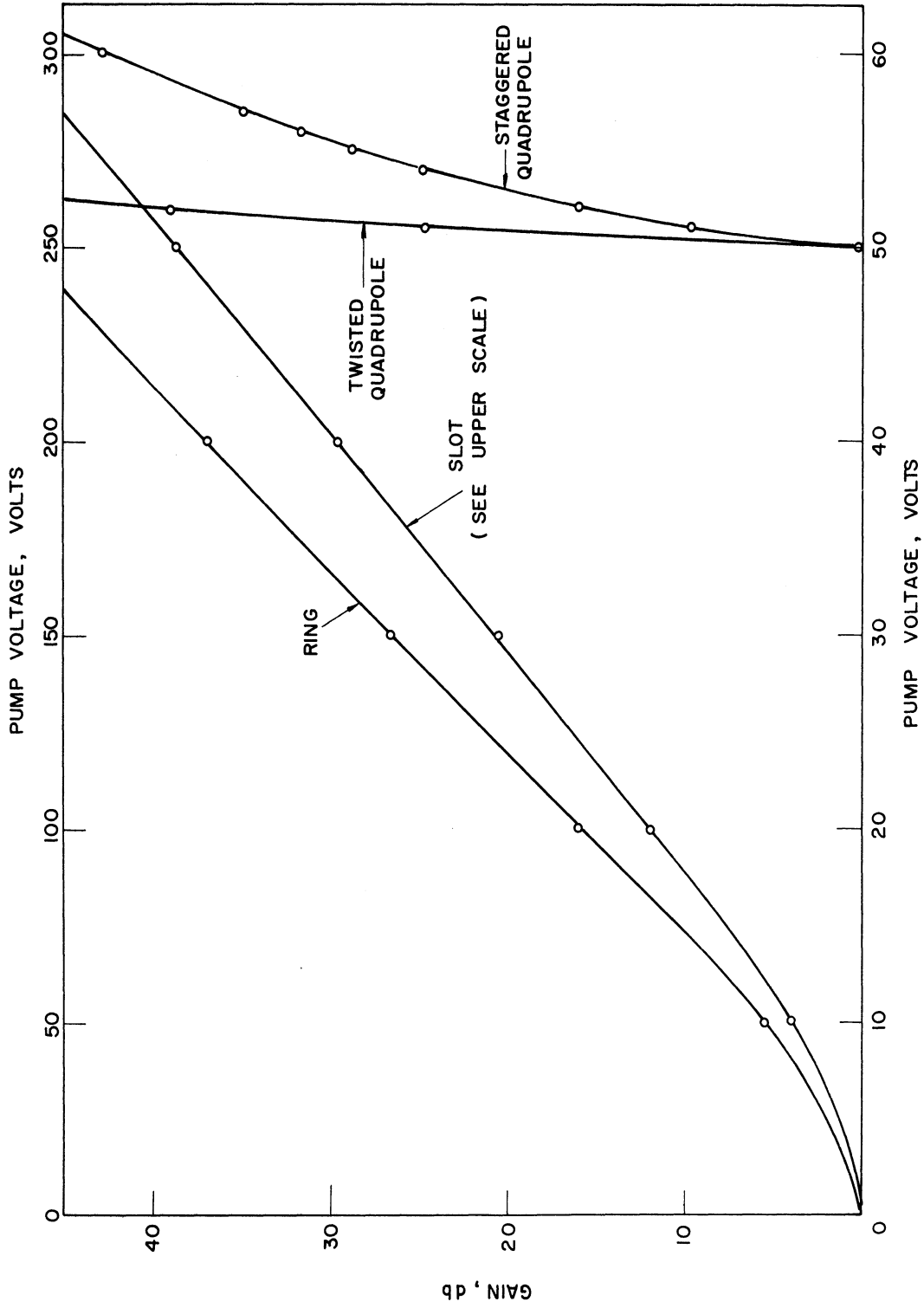


FIG. 4.10 GAIN VS. PUMP VOLTAGE FOR CYCLOTRON-TO-SYNCHRONOUS TYPE OF INTERACTION IN

DIFFERENT PUMP FIELDS FOR $V_0 = 100$ VOLTS, $\beta_c a = 1$, AND $n = 4$.

Table 4.1

Gain Equations for Various Types of Beam Interaction and Different
Types of Pump Fields

Type of Pump Field	Propagation Constant for the Periodic Structure $\beta_q = (2\pi/x_q)$	Type of Mode Copying	Gain (db)	Remark
Staggered Quadrupole	$\beta_q = 2\beta_c$	Cyclotron-Cyclotron	$20 \log^{(1)} \frac{\cosh \frac{\eta V_p n \pi}{\omega_c^2 a^2}}$	
	$\beta_q = 0$	Synchronous-Synchronous	$20 \log \frac{\cosh \frac{2\eta V_p L}{a^2 \omega_c u_o}}$	High gain for synchronous-synchronous amplifier
Twisted Quadrupole	$\beta_q = \beta_c$	Cyclotron-Cyclotron	$20 \log^{(2)} \frac{\cosh \frac{2\eta V_p n \pi}{\omega_c^2 a^2}}$	High gain for cyclotron-cyclotron amplifier
	$\beta_q = 0$	Synchronous-Synchronous	$20 \log \frac{\cosh \frac{\eta V_p L}{a^2 \omega_c u_o}}$	
Ring Structure	$\beta_q = \beta_c$	Cyclotron-Synchronous	$20 \log^{(3)} \frac{\cosh \frac{2\eta V_p n \pi}{\omega^2 a^2}}$	High gain for cyclotron-synchronous amplifier. Single field structure

1. Gordon, E. I., "A Transverse Field Traveling Wave Tube", International Congress on Microwave Tubes, pp. 389-390; 1960.
2. Mao, S. and Siegman, A. E., "Cyclotron Wave Amplification Using Simultaneous R.F.-Coupling and D.C.-Pumping", International Congress on Microwave Tubes, p. 268; 1962.
3. Bass, J. C., "Microwave Amplification in Electrostatic Ring Structures", Proc. I.R.E., vol. 49, p. 1424; 1961.

Table 4.1 (contd)

Type of Pump Field	Propagation Constant for the Periodic Structure $\beta_q = (2\pi/x_q)$	Type of Mode Copying	Gain (db)	Remark
Slot Structure	$\beta_q = \beta_c$	Cyclotron-Synchronous	$20 \log^{(4)} \cosh \frac{\eta\pi V_p}{4V_o \cosh\beta_c a}$	Simple field Structure
	$\beta_q = 2\beta_c$	Cyclotron-Cyclotron	$20 \log \cosh \frac{\eta\pi V_p}{2V_o \cosh(2\beta_c a)}$	

It is noticed that the plot of Eq. 4.61 brings out two important points. First, for a pump voltage below 50 volts (for the set of other parameters chosen), no gain is possible. Beyond this point, the gain rises very rapidly with the increase of the pump voltage. If this were true, then it would be an easy matter to construct a tube with high gain. Two points need investigating. First, is the condition $4M/\beta_c^2 > 1$ physically realizable? Second, since the coupling in this case is between A_1 and A_4 and both of these modes carry positive kinetic power, and as both modes are growing, and power must be delivered to them from the d-c supply, what is the mechanism for this power transfer? The next period shall be devoted to investigate these questions.

Figure 4.11 shows the gain vs. β_q plot for synchronous-to-synchronous wave coupled mode for a set of constant operating conditions. All curves show a decrease in gain as $\beta_c a$ is increased.

Gain is large for small $\beta_c a$. For a constant β_c , small $\beta_c a$ means that a must be small so that the interaction field is strong on the beam.

4. Bass, J. C., "A D.C. Pumped Amplifier with a Two-Dimensional Field Structure", Proc. I.R.E., vol. 49, p. 1959; 1961.

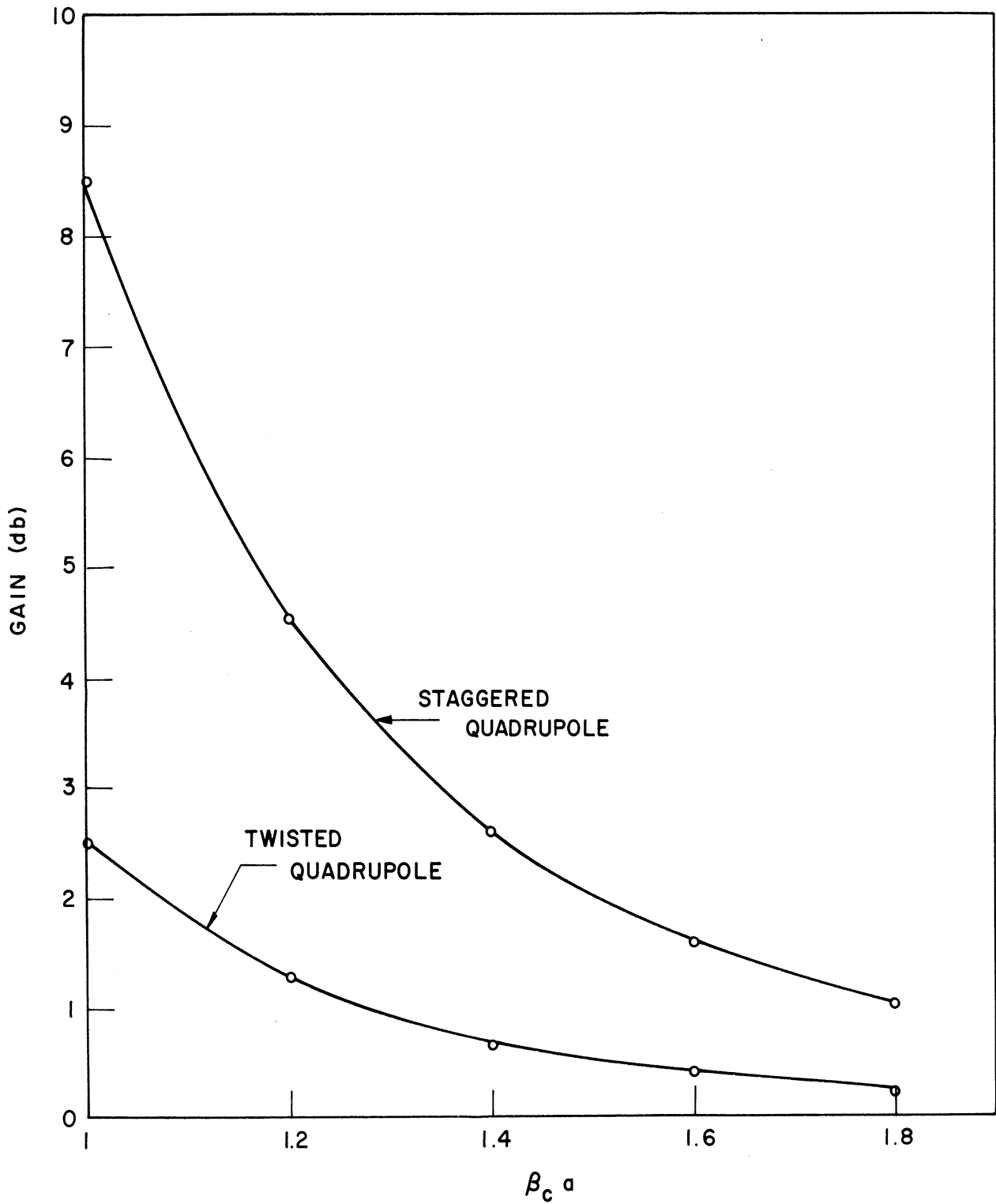


FIG. 4.11 GAIN VS. $\beta_c a$ FOR SYNCHRONOUS-TO-SYNCHRONOUS TYPE OF INTERACTION IN DIFFERENT PUMP FIELDS FOR $V_p/V_0 = 4$, $L = 40$ cm AND $U_0 = 4.2 \times 10^8$ m/sec.

4.4 Future Work. The questions raised in the discussion of the possibility of the coupling between a fast cyclotron wave and the positive synchronous wave are important enough to warrant immediate attention. We shall begin the investigation by correlating the results from other investigators to see whether such criterion has been met. An analysis of the total power relations in the system will be made to visualize the possible energy transfer mechanism.

Other programs will include the continuing search for new pumping field structures, methods of exciting the various modes and eventually to study the noise configurations in the various modes.

5. General Conclusions (C. Yeh)

An experimental low-frequency model of a frequency multiplier has been designed. It is in the process of assembling and final alignment. The device multiplies an input frequency of approximately 700 mc to an output frequency of 2800 mc. A feedback scheme is used to enhance the efficiency.

The analysis of amplitude and phase-modulated traveling-wave amplifiers has been modified to take into account the multivalued nature of the velocity of the electrons when the beam is bunched. Boltzmann's transport equation is used to describe the kinematics of the electron beam.

Difficulty has been encountered in brazing a tungsten helix designed for operation at 30 Gc into a smooth-bore BeO tube. Experimental results indicate that a material which has a higher resiliency than tungsten must be used for the helix.

Coupled-mode theory has been used to analyze the transverse wave d-c pumped quadrupole amplifier. Equations have been derived for the

coupled modes of the different types of quadrupole fields. Gain in various cases are computed and tabulated for easy comparison. An unusual coupling scheme has been uncovered which might result in high gain and a careful evaluation of this mechanism is in progress.

DISTRIBUTION LIST

<u>No. Copies</u>	<u>Agency</u>
3	Chief, Bureau of Ships, Department of the Navy, Washington 25, D. C., Attn: Code 681A1D
1	Chief, Bureau of Ships, Department of the Navy, Washington 25, D. C., Attn: Code 681B2
1	Chief, Bureau of Ships, Department of the Navy, Washington 25, D. C., Attn: Code 687A
3	Chief, Bureau of Ships, Department of the Navy, Washington 25, D. C., Attn: Code 210L
1	Chief, Bureau of Naval Weapons, Department of the Navy, Washington 25, D. C., Attn: Code RAAV-333
1	Chief, Bureau of Naval Weapons, Department of the Navy, Washington 25, D. C., Attn: Code RAAV-61
1	Chief, Bureau of Naval Weapons, Department of the Navy, Washington 25, D. C., Attn: Code RMGA-11
1	Chief, Bureau of Naval Weapons, Department of the Navy, Washington 25, D. C., Attn: Code RMGA-81
1	Director, U. S. Naval Research Laboratory, Washington 25, D. C., Attn: Code 524
2	Director, U. S. Naval Research Laboratory, Washington 25, D. C., Attn: Code 5437
2	Commanding Officer and Director, U. S. Navy Electronics Laboratory, San Diego 52, California, Attn: Code 3260
2	Commander, Aeronautical Systems Division, U. S. Air Force, Wright Patterson Air Force Base, Ohio, Attn: Code ASRPSV-1
2	Commanding Officer, U. S. Army Electronics Research and Development Laboratory, Electron Devices Division, Fort Monmouth, New Jersey
3	Advisory Group on Electron Devices, 346 Broadway, 8th Floor, New York 13, New York
1	Commanding General, Rome Air Development Center, Griffiss Air Force Base, Rome, New York, Attn: RCUIL-2
20	Headquarters, Defense Documentation Center, For Scientific and Technical Information, U. S. Air Force, Cameron Station, Alexandria, Virginia

<u>No. Copies</u>	<u>Agency</u>
1	Microwave Electronics Corporation, 3165 Porter Drive, Stanford Industrial Park, Palo Alto, California
1	Mr. A. G. Peifer, Bendix Corporation, Research Laboratories, Northwestern Highway and 10-1/2 Mile Road, Southfield, Michigan
1	Bendix Corporation, Systems Division, 3300 Plymouth Road, Ann Arbor, Michigan, Attn: Technical Library
1	Litton Industries, 960 Industrial Road, San Carlos, California, Attn: Technical Library
1	Dr. R. P. Wadhwa, Electron Tube Division, Litton Industries, 960 Industrial Way, San Carlos, California
1	The University of Michigan, Willow Run Laboratories, Ypsilanti, Michigan, Attn: Dr. J. T. Wilson
1	Microwave Associates, Burlington, Massachusetts, Attn: Technical Library
1	Microwave Electronic Tube Company, Inc., Salem, Massachusetts, Attn: Technical Library
1	Radio Corporation of America, Power Tube Division, Harrison, New Jersey
1	Raytheon Company, Burlington, Massachusetts, Attn: Technical Library
1	S-F-D Laboratories, 800 Rahway Avenue, Union, New Jersey, Attn: Technical Library
1	Tucor, Inc., 18 Marshall Street, South Norwalk, Connecticut, Attn: Technical Library
1	Dr. Walter M. Nunn, Jr., Electrical Engineering Department, Tulane University, New Orleans, Louisiana
1	Westinghouse Electric Corporation, P. O. Box 284, Elmira, New York, Attn: Technical Library
1	Bendix Corporation, Red Bank Division, Eatontown, New Jersey, Attn Dr. James Palmer
1	Mr. A. Weglein, Hughes Aircraft Company, Microwave Tube Division, 11105 South LaCienaga Blvd., Los Angeles 9, California

<p>AD</p> <p>The University of Michigan, Electron Physics Laboratory, Ann Arbor, Michigan. BASIC RESEARCH IN MICROWAVE DEVICES AND QUANTUM ELECTRONICS, by H. K. Detweiler, et. al. March, 1964, 75 pp. incl. illus. (Project Serial No. SRO080301, Task 9391, Contract No. N0bsr-89274)</p> <p><u>Generation and Amplification of Coherent Electromagnetic Energy in the Millimeter and Submillimeter Wavelength Region</u></p> <p>An experimental low-frequency model of the frequency multiplier has been designed. A scheme of feedback to enhance the transfer efficiency is included. The tube is in the final stage of assembly and alignment.</p> <p>Difficulties in loading a helix designed to operate at 30 Gc into a BeO tube have not been fully resolved. Experimental data indicates that a material having a higher resiliency than tungsten should be used for the helix.</p> <p><u>Analysis of Amplitude and Phase Modulated Traveling-Wave Amplifiers</u></p> <p>The analysis of the operation of the TWA with a multi-frequency input has been extended to account for the multivalued nature of the electron velocity in the beam. Boltzmann's transport equation is used to describe the kinematics of the electron beam.</p> <p><u>Study of a D-c Pumped Quadrupole Amplifier</u></p> <p>A comprehensive study of the coupling mechanism between the various modes of operation of a d-c pumped transverse wave device has been made by means of the coupled-mode theory. Equations for the gain for the various modes and different pump fields are computed and compared.</p>	<p>UNCLASSIFIED</p> <ol style="list-style-type: none"> 1. General Introduction. 2. Generation and Amplification of Coherent Electromagnetic Energy in the Millimeter and Submillimeter Wavelength Region. 3. Analysis of Amplitude and Phase Modulated Traveling-Wave Amplifiers. 4. Study of a D-c Pumped Quadrupole Amplifier. 5. General Conclusions. I. Detweiler, H. K. II. El-Shandawily, M. E. III. Ho, B. IV. Rok, G. V. Rowe, J. E. VI. Yeh, C. 	<p>AD</p> <p>The University of Michigan, Electron Physics Laboratory, Ann Arbor, Michigan. BASIC RESEARCH IN MICROWAVE DEVICES AND QUANTUM ELECTRONICS, by H. K. Detweiler, et. al. March, 1964, 75 pp. incl. illus. (Project Serial No. SRO080301, Task 9391, Contract No. N0bsr-89274)</p> <p><u>Generation and Amplification of Coherent Electromagnetic Energy in the Millimeter and Submillimeter Wavelength Region</u></p> <p>An experimental low-frequency model of the frequency multiplier has been designed. A scheme of feedback to enhance the transfer efficiency is included. The tube is in the final stage of assembly and alignment.</p> <p>Difficulties in loading a helix designed to operate at 30 Gc into a BeO tube have not been fully resolved. Experimental data indicates that a material having a higher resiliency than tungsten should be used for the helix.</p> <p><u>Analysis of Amplitude and Phase Modulated Traveling-Wave Amplifiers</u></p> <p>The analysis of the operation of the TWA with a multi-frequency input has been extended to account for the multivalued nature of the electron velocity in the beam. Boltzmann's transport equation is used to describe the kinematics of the electron beam.</p> <p><u>Study of a D-c Pumped Quadrupole Amplifier</u></p> <p>A comprehensive study of the coupling mechanism between the various modes of operation of a d-c pumped transverse wave device has been made by means of the coupled-mode theory. Equations for the gain for the various modes and different pump fields are computed and compared.</p>	<p>UNCLASSIFIED</p> <ol style="list-style-type: none"> 1. General Introduction. 2. Generation and Amplification of Coherent Electromagnetic Energy in the Millimeter and Submillimeter Wavelength Region. 3. Analysis of Amplitude and Phase Modulated Traveling-Wave Amplifiers. 4. Study of a D-c Pumped Quadrupole Amplifier. 5. General Conclusions. I. Detweiler, H. K. II. El-Shandawily, M. E. III. Ho, B. IV. Rok, G. V. Rowe, J. E. VI. Yeh, C.
<p>AD</p> <p>The University of Michigan, Electron Physics Laboratory, Ann Arbor, Michigan. BASIC RESEARCH IN MICROWAVE DEVICES AND QUANTUM ELECTRONICS, by H. K. Detweiler, et. al. March, 1964, 75 pp. incl. illus. (Project Serial No. SRO080301, Task 9391, Contract No. N0bsr-89274)</p> <p><u>Generation and Amplification of Coherent Electromagnetic Energy in the Millimeter and Submillimeter Wavelength Region</u></p> <p>An experimental low-frequency model of the frequency multiplier has been designed. A scheme of feedback to enhance the transfer efficiency is included. The tube is in the final stage of assembly and alignment.</p> <p>Difficulties in loading a helix designed to operate at 30 Gc into a BeO tube have not been fully resolved. Experimental data indicates that a material having a higher resiliency than tungsten should be used for the helix.</p> <p><u>Analysis of Amplitude and Phase Modulated Traveling-Wave Amplifiers</u></p> <p>The analysis of the operation of the TWA with a multi-frequency input has been extended to account for the multivalued nature of the electron velocity in the beam. Boltzmann's transport equation is used to describe the kinematics of the electron beam.</p> <p><u>Study of a D-c Pumped Quadrupole Amplifier</u></p> <p>A comprehensive study of the coupling mechanism between the various modes of operation of a d-c pumped transverse wave device has been made by means of the coupled-mode theory. Equations for the gain for the various modes and different pump fields are computed and compared.</p>	<p>UNCLASSIFIED</p> <ol style="list-style-type: none"> 1. General Introduction. 2. Generation and Amplification of Coherent Electromagnetic Energy in the Millimeter and Submillimeter Wavelength Region. 3. Analysis of Amplitude and Phase Modulated Traveling-Wave Amplifiers. 4. Study of a D-c Pumped Quadrupole Amplifier. 5. General Conclusions. I. Detweiler, H. K. II. El-Shandawily, M. E. III. Ho, B. IV. Rok, G. V. Rowe, J. E. VI. Yeh, C. 	<p>AD</p> <p>The University of Michigan, Electron Physics Laboratory, Ann Arbor, Michigan. BASIC RESEARCH IN MICROWAVE DEVICES AND QUANTUM ELECTRONICS, by H. K. Detweiler, et. al. March, 1964, 75 pp. incl. illus. (Project Serial No. SRO080301, Task 9391, Contract No. N0bsr-89274)</p> <p><u>Generation and Amplification of Coherent Electromagnetic Energy in the Millimeter and Submillimeter Wavelength Region</u></p> <p>An experimental low-frequency model of the frequency multiplier has been designed. A scheme of feedback to enhance the transfer efficiency is included. The tube is in the final stage of assembly and alignment.</p> <p>Difficulties in loading a helix designed to operate at 30 Gc into a BeO tube have not been fully resolved. Experimental data indicates that a material having a higher resiliency than tungsten should be used for the helix.</p> <p><u>Analysis of Amplitude and Phase Modulated Traveling-Wave Amplifiers</u></p> <p>The analysis of the operation of the TWA with a multi-frequency input has been extended to account for the multivalued nature of the electron velocity in the beam. Boltzmann's transport equation is used to describe the kinematics of the electron beam.</p> <p><u>Study of a D-c Pumped Quadrupole Amplifier</u></p> <p>A comprehensive study of the coupling mechanism between the various modes of operation of a d-c pumped transverse wave device has been made by means of the coupled-mode theory. Equations for the gain for the various modes and different pump fields are computed and compared.</p>	<p>UNCLASSIFIED</p> <ol style="list-style-type: none"> 1. General Introduction. 2. Generation and Amplification of Coherent Electromagnetic Energy in the Millimeter and Submillimeter Wavelength Region. 3. Analysis of Amplitude and Phase Modulated Traveling-Wave Amplifiers. 4. Study of a D-c Pumped Quadrupole Amplifier. 5. General Conclusions. I. Detweiler, H. K. II. El-Shandawily, M. E. III. Ho, B. IV. Rok, G. V. Rowe, J. E. VI. Yeh, C.

<p>AD</p> <p>The University of Michigan, Electron Physics Laboratory, Ann Arbor, Michigan. BASIC RESEARCH IN MICROWAVE DEVICES AND QUANTUM ELECTRONICS, by H. K. Detweiler, et. al. March, 1964, 75 pp. incl. illus. (Project Serial No. SRO080301, Task 9291, Contract No. N0bsr-89274)</p> <p>Generation and Amplification of Coherent Electromagnetic Energy in the Millimeter and Submillimeter Wavelength Region</p> <p><u>Analysis of Amplitude and Phase Modulated Traveling-Wave Amplifiers</u></p> <p>An experimental low-frequency model of the frequency multiplier has been designed. A scheme of feedback to enhance the transfer efficiency is included. The tube is in the final stage of assembly and alignment.</p> <p>Difficulties in loading a helix designed to operate at 30 Gc into a BeO tube have not been fully resolved. Experimental data indicates that a material having a higher resiliency than tungsten should be used for the helix.</p> <p><u>Analysis of Amplitude and Phase Modulated Traveling-Wave Amplifiers</u></p> <p>The analysis of the operation of the TWA with a multi-frequency input has been extended to account for the multivalued nature of the electron velocity in the beam. Boltzmann's transport equation is used to describe the kinematics of the electron beam.</p> <p><u>Study of a D-c Pumped Quadrupole Amplifier</u></p> <p>A comprehensive study of the coupling mechanism between the various modes of operation of a d-c pumped transverse wave device has been made by means of different pump fields are computed and compared.</p>	<p>UNCLASSIFIED</p> <ol style="list-style-type: none"> 1. General Introduction. 2. Generation and Amplification of Coherent Electromagnetic Energy in the Millimeter and Submillimeter Wavelength Region. 3. Analysis of Amplitude and Phase Modulated Traveling-Wave Amplifiers. 4. Study of a D-c Pumped Quadrupole Amplifier. 5. General Conclusions. <ol style="list-style-type: none"> I. Detweiler, H. K. II. El-Shandawily, M. E. III. Hok, G. IV. Rowe, J. E. VI. Yeh, C. 	<p>AD</p> <p>The University of Michigan, Electron Physics Laboratory, Ann Arbor, Michigan. BASIC RESEARCH IN MICROWAVE DEVICES AND QUANTUM ELECTRONICS, by H. K. Detweiler, et. al. March, 1964, 75 pp. incl. illus. (Project Serial No. SRO080301, Task 9291, Contract No. N0bsr-89274)</p> <p>Generation and Amplification of Coherent Electromagnetic Energy in the Millimeter and Submillimeter Wavelength Region</p> <p><u>Analysis of Amplitude and Phase Modulated Traveling-Wave Amplifiers</u></p> <p>An experimental low-frequency model of the frequency multiplier has been designed. A scheme of feedback to enhance the transfer efficiency is included. The tube is in the final stage of assembly and alignment.</p> <p>Difficulties in loading a helix designed to operate at 30 Gc into a BeO tube have not been fully resolved. Experimental data indicates that a material having a higher resiliency than tungsten should be used for the helix.</p> <p><u>Analysis of Amplitude and Phase Modulated Traveling-Wave Amplifiers</u></p> <p>The analysis of the operation of the TWA with a multi-frequency input has been extended to account for the multivalued nature of the electron velocity in the beam. Boltzmann's transport equation is used to describe the kinematics of the electron beam.</p> <p><u>Study of a D-c Pumped Quadrupole Amplifier</u></p> <p>A comprehensive study of the coupling mechanism between the various modes of operation of a d-c pumped transverse wave device has been made by means of the coupled-mode theory. Equations for the gain for the various modes and different pump fields are computed and compared.</p>	<p>UNCLASSIFIED</p> <ol style="list-style-type: none"> 1. General Introduction. 2. Generation and Amplification of Coherent Electromagnetic Energy in the Millimeter and Submillimeter Wavelength Region. 3. Analysis of Amplitude and Phase Modulated Traveling-Wave Amplifiers. 4. Study of a D-c Pumped Quadrupole Amplifier. 5. General Conclusions. <ol style="list-style-type: none"> I. Detweiler, H. K. II. El-Shandawily, M. E. III. Hok, G. IV. Rowe, J. E. VI. Yeh, C.
<p>AD</p> <p>The University of Michigan, Electron Physics Laboratory, Ann Arbor, Michigan. BASIC RESEARCH IN MICROWAVE DEVICES AND QUANTUM ELECTRONICS, by H. K. Detweiler, et. al. March, 1964, 75 pp. incl. illus. (Project Serial No. SRO080301, Task 9291, Contract No. N0bsr-89274)</p> <p>Generation and Amplification of Coherent Electromagnetic Energy in the Millimeter and Submillimeter Wavelength Region</p> <p><u>Analysis of Amplitude and Phase Modulated Traveling-Wave Amplifiers</u></p> <p>An experimental low-frequency model of the frequency multiplier has been designed. A scheme of feedback to enhance the transfer efficiency is included. The tube is in the final stage of assembly and alignment.</p> <p>Difficulties in loading a helix designed to operate at 30 Gc into a BeO tube have not been fully resolved. Experimental data indicates that a material having a higher resiliency than tungsten should be used for the helix.</p> <p><u>Analysis of Amplitude and Phase Modulated Traveling-Wave Amplifiers</u></p> <p>The analysis of the operation of the TWA with a multi-frequency input has been extended to account for the multivalued nature of the electron velocity in the beam. Boltzmann's transport equation is used to describe the kinematics of the electron beam.</p> <p><u>Study of a D-c Pumped Quadrupole Amplifier</u></p> <p>A comprehensive study of the coupling mechanism between the various modes of operation of a d-c pumped transverse wave device has been made by means of different pump fields are computed and compared.</p>	<p>UNCLASSIFIED</p> <ol style="list-style-type: none"> 1. General Introduction. 2. Generation and Amplification of Coherent Electromagnetic Energy in the Millimeter and Submillimeter Wavelength Region. 3. Analysis of Amplitude and Phase Modulated Traveling-Wave Amplifiers. 4. Study of a D-c Pumped Quadrupole Amplifier. 5. General Conclusions. <ol style="list-style-type: none"> I. Detweiler, H. K. II. El-Shandawily, M. E. III. Hok, G. IV. Rowe, J. E. VI. Yeh, C. 	<p>AD</p> <p>The University of Michigan, Electron Physics Laboratory, Ann Arbor, Michigan. BASIC RESEARCH IN MICROWAVE DEVICES AND QUANTUM ELECTRONICS, by H. K. Detweiler, et. al. March, 1964, 75 pp. incl. illus. (Project Serial No. SRO080301, Task 9291, Contract No. N0bsr-89274)</p> <p>Generation and Amplification of Coherent Electromagnetic Energy in the Millimeter and Submillimeter Wavelength Region</p> <p><u>Analysis of Amplitude and Phase Modulated Traveling-Wave Amplifiers</u></p> <p>An experimental low-frequency model of the frequency multiplier has been assigned. A scheme of feedback to enhance the transfer efficiency is included. The tube is in the final stage of assembly and alignment.</p> <p>Difficulties in loading a helix designed to operate at 30 Gc into a BeO tube have not been fully resolved. Experimental data indicates that a material having a higher resiliency than tungsten should be used for the helix.</p> <p><u>Analysis of Amplitude and Phase Modulated Traveling-Wave Amplifiers</u></p> <p>The analysis of the operation of the TWA with a multi-frequency input has been extended to account for the multivalued nature of the electron velocity in the beam. Boltzmann's transport equation is used to describe the kinematics of the electron beam.</p> <p><u>Study of a D-c Pumped Quadrupole Amplifier</u></p> <p>A comprehensive study of the coupling mechanism between the various modes of operation of a d-c pumped transverse wave device has been made by means of the coupled-mode theory. Equations for the gain for the various modes and different pump fields are computed and compared.</p>	<p>UNCLASSIFIED</p> <ol style="list-style-type: none"> 1. General Introduction. 2. Generation and Amplification of Coherent Electromagnetic Energy in the Millimeter and Submillimeter Wavelength Region. 3. Analysis of Amplitude and Phase Modulated Traveling-Wave Amplifiers. 4. Study of a D-c Pumped Quadrupole Amplifier. 5. General Conclusions. <ol style="list-style-type: none"> I. Detweiler, H. K. II. El-Shandawily, M. E. III. Hok, G. IV. Rowe, J. E. VI. Yeh, C.

UNIVERSITY OF MICHIGAN



3 9015 02526 1671